LIQUID CRYSTALS, 1994, VOL. 16, NO. 1, 1–31

Invited Article

Polymer-dispersed liquid crystals
From the nematic curvilinear aligned phase to ferroelectric films†

by HEINZ-S. KITZEROW
Iwan-N.-Stranski-Institut, Technische Universität Berlin,
Sekr. ER11, Strasse des 17. Juni 135, 10623 Berlin, Germany

(*Received March 1993; accepted 26 June 1993*)

Polymer-dispersed liquid crystals (PDLC) are widely used for electro-optic applications such as flexible displays, privacy windows or projection displays. Besides these applications, the confinement of a liquid crystal to small cavities is of fundamental interest. The present paper contains a review of the work on nematic and cholesteric PDLCs. Moreover, some very recent developments are summarized such as the use of ferroelectric liquid crystals for PDLC applications.

1. Introduction

Since the discovery of liquid crystals more than 100 years ago [1], dispersions of liquid crystal droplets in an isotropic liquid have attracted the attention of many scientists. By means of optical polarization microscopy, Lehmann [2] and Friedel [3] extensively studied the behaviour of such droplets at the clearing point of liquid crystals. Among the first applications of liquid crystal droplets was the use of encapsulated thermochromic cholesteric liquid crystals as thermometers, due to the temperature dependence of the selective reflection wavelength [4].

Today, liquid crystals are important because of their application in flat panel displays. However, in the past decade *dispersions* of liquid crystals have become interesting due to their electro-optic applications [5, 6]. Fergason [7] and Doane *et al.* [8], proposed the use of nematic droplets which are embedded in a polymer film (see figure 1). These polymer-dispersed liquid crystals (PDLC) can be switched between a translucent 'off' state and a transparent 'on' state due to mismatching or matching of the refractive indices. In the field-off state, surface anchoring causes a non-uniform director field within the droplets, the film scatters light due to mismatching between the effective refractive index n_{eff} of the liquid crystal and the refractive index n_p of the polymer. In the field-on state, the director is aligned along the field direction, i.e. $n_{eff} = n_o$, and for normal light incidence the film becomes transparent if the ordinary refractive index n_o of the liquid crystal is equal to n_p. In comparison with conventional liquid crystal displays, these films are flexible and very easy to prepare, since no orienting glass plates are required. In addition, they show a high transmittance because no polarizers are needed. Owing to these advantages, PDLC films are used for privacy windows and display applications (see figure 2).

More recently, Crooker and Yang [9] have developed a reflective colour display using cholesteric PDLCs. In this device, the selective reflection of highly chiral liquid

† Plenary Lecture at the European Conference on Liquid Crystals, Films (CH), March 1993.

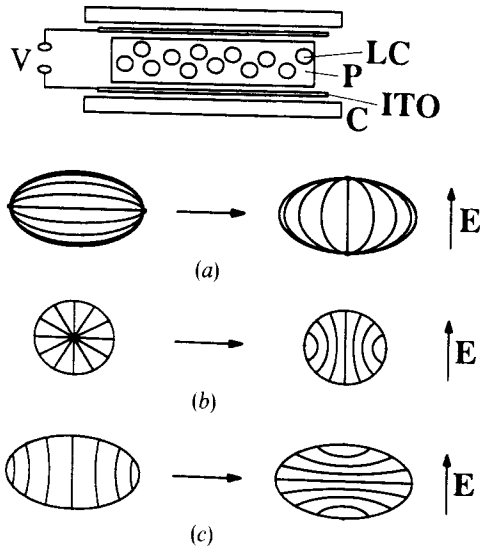

Figure 1. Top: Schematic presentation of a nematic PDLC display (P), polymer; LC, liquid crystal; ITO, transparent conducting layer; C, cover sheet. Below: field-induced changes of the director field within a droplet under different conditions. (*a*) Reorientation of a bipolar structure in elliptical droplets (planar anchoring, $\varepsilon_a > 0$). (*b*) Discontinuous transition from a radial to an axial structure (perpendicular anchoring, $\varepsilon_a > 0$). (*c*) Reverse mode (transparent field-off state and opaque field-on state): reorientation of an axial structure in elliptical cavities (perpendicular anchoring, $\varepsilon_a < 0$).

crystals with negative dielectric anisotropy is used to switch from a field-off state without reflectivity to a coloured reflecting state. The use of chiral liquid crystals in PDLC devices has also been extended to smectic liquid crystals [10] which are known for fast switching effects due to ferroelectricity [11].

With respect to the history of the electro-optic application of liquid crystals, it is interesting to note that the first displays made use of light scattering effects, such as field-induced electro-hydrodynamic instabilities or the phase change effect [12]. Electro-optic applications using refractive index matching or mismatching of liquid crystals contained in micrometer sized inclusions in a non-absorbing solid have also been suggested [13]. In contrast to these effects, the commonly used twisted nematic (TN) [14] and supertwisted nematic (STN) cells [12] make use of a waveguiding effect, and in ferroelectric liquid crystal (FLC) displays [11], the liquid crystal layer is used as a tunable wave plate. For these latter effects, crossed polarizers must be used in order to achieve suitable optical contrast and much effort has gone into producing a defect free orientation of the liquid crystal by surface treatment of the glass substrate.

The development of PDLC displays caused a revival of electro-optic scattering effects and initially seemed to make sophisticated surface treatments obsolete. However, further studies have shown that the properties of certain PDLC devices may be improved by a prealignment of the liquid crystal in the PDLC film which can be achieved by mechanical stress or by applying external fields during sample preparation [15, 16]. Such a preorientation is also a condition for the use of fast-switching ferroelectric liquid crystals in PDLC displays [10], and most recently it has even been suggested that the preparation and the alignment of conventional liquid crystal

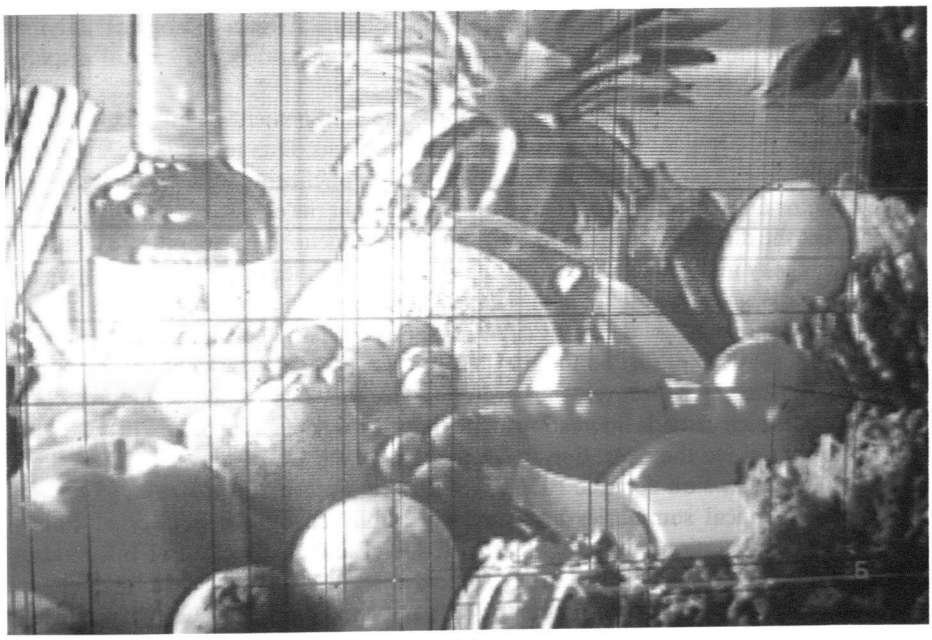

(*a*)

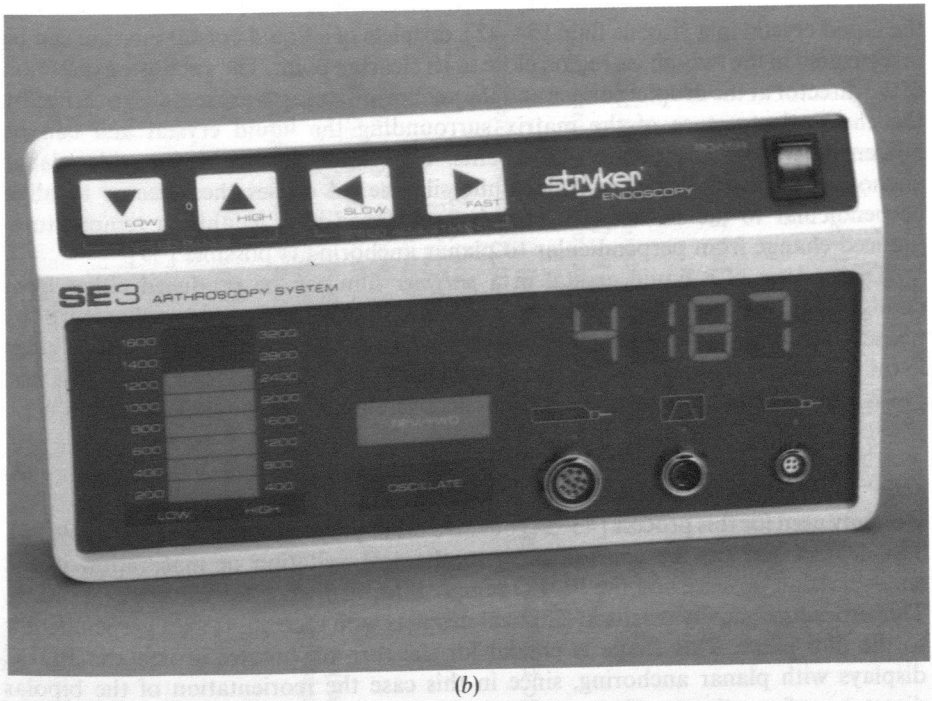

(*b*)

Figure 2. PDLC applications. (*a*) Projection display [courtesy of Dr T. Gunjima, Asahi-glass, Tokyo, Japan], (*b*) reflective display [courtesy of Dr P. S. Drzaic, Raychem Corp., Menlo Park, California, USA].

displays can be improved by incorporating small amounts of a mesogenic polymer network in the liquid crystal (volume-stabilized ferroelectric liquid crystal displays [17]).

Beyond the aspects of PDLC applications, the confinement of liquid crystals to small cavities involves interesting fundamental problems. Due to the large surface to volume ratio of a liquid crystal microdroplet, surface anchoring governs the structure of the director field. In addition, surface terms appear in the elastic free energy [18, 19] which affect the director field even in the limit of zero anchoring strength [20]. Surface interactions may induce nematic order in a thin surface layer many degrees above the clearing point of the liquid crystal [21, 22]; the nematic–isotropic transition can become continuous below a critical cavity size [23–25]; and certain phases such as the smectic twisted grain boundary (TGB) phases—may be stabilized by the confinement [26, 27]. Moreover, the surface anchoring causes defect structures of the director field which provide interesting analogies to other defects in nature [28–30], but are also essential for the operation and dynamics of PDLC displays.

Excellent reviews on nematic PDLCs have been given by Doane *et al.* [5, 6], and up-to-date technical summaries are regularly published by the Society of Photo-Optical Instrumentation Engineers (SPIE) [31–32] and the Society of Information Display (SID) [33]. In the present article, preparation methods for PDLC displays are reviewed (§ 2), recent advances in nematic (§ 3) and cholesteric PDLCs (§ 4) are briefly summarized, and new trends making use of *chiral smectic* PDLCs are discussed in § 5.

2. Preparation

For basic investigations, liquid crystal droplets can be easily studied by dispersing the liquid crystal in a viscous fluid [34–42]; droplets of a liquid crystal mixture can be investigated in the two-phase region close to its clearing point. The anchoring direction of the director at the droplet surface and the anchoring strength are mainly governed by the chemical structure of the matrix surrounding the liquid crystal and can be influenced by the addition of surfactants. Glycerol is known to provide planar anchoring for most liquid crystals, while silicone oil causes the director to align perpendicular to the surface [38]. In glycerol doped with lecithin, a temperature-induced change from perpendicular to planar anchoring is possible [39].

Dispersions of a liquid crystal in a *polymer* film can be produced either from emulsions [7] (by encapsulation of the liquid crystal with water soluble polymers) or by phase separation [8]. An overview of the polymers used for different techniques is given in the table. For historical reasons, the name nematic curvilinear aligned phase (NCAP) [7] is restricted to systems prepared by encapsulation. Poly(vinyl-alcohol) (PVA)

$$\left(-CH_2-\underset{\displaystyle OH}{\underset{|}{CH}}-\right)_p \qquad (1)$$

is mainly used for this process [43–54] but also other polymers have been tried [49, 55]. The droplet size can be controlled by mechanical agitation or maceration in the emulsification process, and the PDLC sample is formed when the solvent evaporates. This procedure usually results in elliptical droplets with their short axes perpendicular to the film plane. This shape is crucial for the turn-off process in nematic PDLC displays with planar anchoring, since in this case the reorientation of the bipolar director configuration (see figure 1 (*a*)) is due to the decrease of the elastic deformation energy when the symmetry axis of the director field aligns along the major axis of the droplet.

Frequently used matrix materials for different preparation methods.

	Planar anchoring	Perpendicular anchoring
Dispersion in viscous fluids	Glycerol [34–38] Glycerol/lecithin [39]	Glycerol/water/polyethylene glycol [34] Glycerol/lecithin [39] Glycerol/CTAB [34] Water [40, 41] Silicon oil [38, 42]
NCAP	PVA [7, 43–53] PVA/Glycerol [54] Polyurethane latex [49] Gelatin [55]	
PIPS Thermosetting systems)	Epon-828/amine curing agent [8, 56–59] Epon-828/Capcure 3-800 [57, 60] Epon-812/Capcure 3-800 [57, 60, 61] Epon-828/MK-107/Capcure 3-800 [62–66] Epon-828/Epon-165/Capcure 3-800 [67] Epoxy side chain polymers [68, 69] Bostik 'Saldo rapido' [70, 71] Devcon '5-Minute-Epoxy' [72]	Tu50A (Conap Inc.) [56, 73, 74], other polyurethanes [72]
PIPS (photo-polymerization)	Trimethylolpropane/tri-(2-mercaptopropanoate)/allyl compounds [75–79, 16] Vinyl compounds [80] Polyester resins [81, 82] Urethane and urethane-acrylate mixtures [82] NOA65 [45, 15, 61, 72, 83–89] Diurethane/diacrylate-photomer 6008 [72]	NOA65 (high T) [92]
TIPS	Poly(carbonate) [60] Poly(vinylformal) [60] Poly(vinylbutyral) [9, 166, 167] PMMA [70] NF-100 [94]	PIBMA [95]
SIPS	PMMA [62, 96–98] PMMA/Fluoropolymer [99] PVC/Vinylacetate [97] NF-100 [94, 98, 100] Poly(vinylpyrrolidone) [101] Poly(vinylformal) [102] Polystyrene [103]	

As an alternative, several techniques of controlled phase separation have been developed. For polymerization induced phase separation (PIPS) the liquid crystal is homogeneously mixed with polymer precursors and phase separation takes place during the polymerization. In thermosets [56–74], the polymer may be formed by an *epoxy resin*, such as the diglycidylether of bisphenol A (Epon-828, Shell Chemical Co., Houston, U.S.A.)

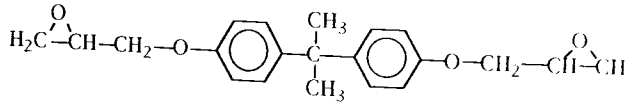

(2)

or an analogous saturated compound such as (Epon-165)

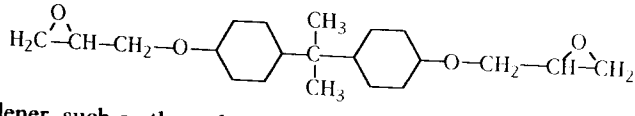

(3)

and a hardener, such as the polymercaptane Capcure 3-800

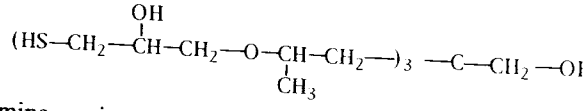

(4)

or a polyamine curing agent. The aim of mixing the compound (2) with an aliphatic compound, such as (3) or cyclohexanedimethanol diglycidylether (MK-107, Wilmington Chemical Co.) [62] is to achieve refractive index matching. *Mesogenic* amines

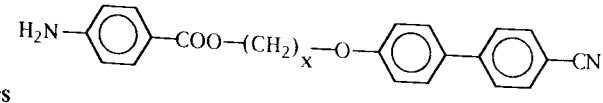

(5)

and diamines

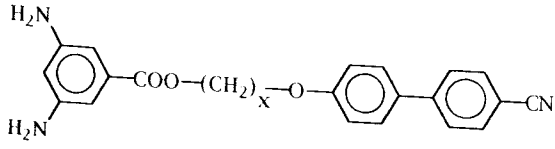

(6)

may be used as curing agents for epoxy resins to obtain side chain polymers and cross-linked networks, respectively [68, 69]. Such oriented liquid crystal polymers may be used instead of an isotropic polymer matrix to obtain haze-free light shutters [68]. While epoxy resins are known to provide planar anchoring of the director at the droplet surface, *polyurethanes*, such as Tu 50A (Conap Inc., Buffalo, N.Y.) are used to achieve perpendicular anchoring [56, 73–74].

A very handy method of PIPS utilizes the photopolymerization of *UV-curable adhesives* [75–92]. In this process, the start of the polymerization is very accurately defined, the reaction can be slowed by interrupting the UV illumination, and the polymerization rate can easily be varied by the light intensity. The most commonly used thiol-ene photomer, NOA-65 (Norland Inc., New Brunswick, N.J., USA), is a mixture of trimethylolpropane diallyl ether, trimethylolpropane tris thiol, isophorone di-isocyanate ester, and benzophenone photoinitiator [85]. For UV-cured PIPS, special liquid crystals have been developed in order to obtain the refractive index matching, to optimize the phase separation, and to enhance the UV-stability of the liquid crystal [88–90]. In addition, the use of chemical accelerators for the curing

process has been demonstrated to improve the optical attenuation of PDLC films [93]. In principle, UV-curable precursors may also be polymerized by electron beams instead of using UV light [83].

Besides the PIPS technique, phase separation may be achieved by cooling a homogeneous mixture of the liquid crystal and a thermoplastic polymer (thermally induced phase separation, TIPS [60, 70, 94–95]) or by controlled solvent evaporation from a solution of the liquid crystal and the polymer (solvent-induced phase separation, SIPS [62, 96–103]). For the latter two methods, mainly *vinyl polymers*

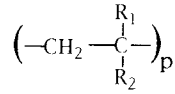

(7)

such as poly(methyl methacrylate) (PMMA: $R_1 = CH_3$, $R_2 = CO_2CH_3$), poly(vinyl-acetate) (PVAc: $R_1 = H$, $R_2 = OOC\text{-}CH_3$), poly(vinyl-chloride) (PVC: $R_1 = H$, $R_2 = Cl$) and polystyrene ($R_1 = H$, $R_2 = C_6H_5$), or vinyl polymers with cyclic acetal groups, for example, polyvinylformal (PVF) and polyvinylbutyral (PVB)

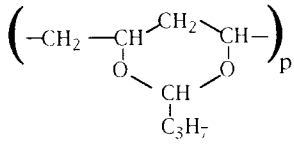

(8)

or polyesters such as polycarbonate

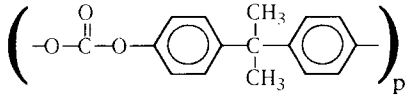

(9)

have been used. While these polymers provide planar anchoring, poly(isobutyl methacrylate) (PIBMA) is known to cause perpendicular anchoring [95].

Variations of PDLC displays are the recently developed *anisotropic gels* [104–108] or *liquid crystal-dispersed polymers* [109], where a small amount (typically a few per cent) of a mesogenic polymer precursor is dissolved in a nematic [104, 105, 109] or cholesteric [106–108] liquid crystal and cross-linked by photopolymerization. These systems are useful to build transmissive displays basing on scattering effects [104, 105], bistable reflective colour displays [107], or haze-free light shutters [108]. Liquid crystalline diacrylates like

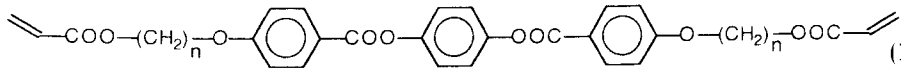

(10)

or the mesogenic 4,4′-bisacryloylbiphenyl

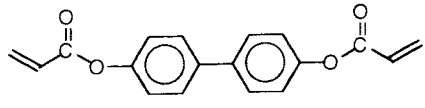

(11)

have been used to form the polymer network in these devices. Most recently, *glass-dispersed liquid crystal* systems have been developed [110, 111]: using sol-gel processes, liquid crystal droplets have been trapped into silica gel.

Turning to the liquid crystals, *normal-mode* PDLC displays require a nematic liquid crystal with *positive dielectric anisotropy* ε_a. Mainly alkylcyanobiphenyls (for example, 5-CBP, 7-CBP [57]), alkyloxycyanobiphenyls (for example, 6-O-CBP [57]), or eutectic

mixtures of similar compounds, such as E7, E8, E9 (Merck Ltd, Poole, England), ZLI 1840 (Merck, Darmstadt, Germany), or RO-TN 404 (Hoffmann-La Roche, Basel, Switzerland) have been studied. For photopolymerization, special liquid crystal mixtures and polymers have been developed in order to reduce the solubility of the prepolymer in the liquid crystal droplets [88], to increase the birefringence [89], and to enhance the UV stability of the liquid crystal [112]. *Reverse mode* displays (which are transparent in the field-off state and opaque in the field-on state), require nematic liquid crystals with *negative dielectric anisotropy* ε_a [113] or *dual-frequency addressable liquid crystals* [84] in order to reorient the liquid crystal from a uniform alignment perpendicular to the film surface to a planar alignment perpendicular to the field (see figure 1 (*c*)). The latter compounds, which show $\varepsilon_a > 0$ for low frequencies and $\varepsilon_a < 0$ for high frequencies, are also useful for reducing the switching times in normal mode displays [87], for thermoelectro-optic switches [94] and for basic research [114]. For *reflective colour displays* [9], nematic liquid crystals with negative dielectric anisotropy have been chiralized by the addition of *chiral dopants* with high helical twisting power, such as CE2 (Merck Ltd., Poole, England)

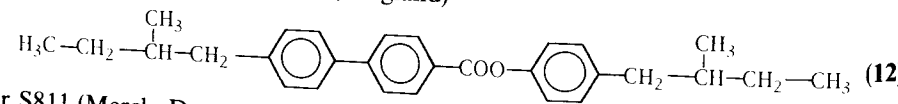

(12)

or S811 (Merck, Darmstadt, Germany).

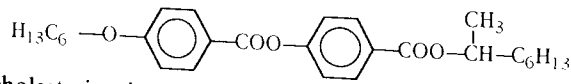

(13)

For aliphatic cholesteric mixtures with negative dielectric anisotropy, PVB (compound (**8**)) has been found to give better phase separation than linear vinyl polymers [9].

For polymer-dispersed ferroelectric liquid crystal light shutters, the chiral smectic compound (**14**)

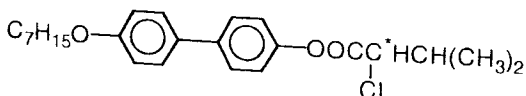

(14)

[10, 115] and room-temperature mixtures of this compound with a non-chiral smectic liquid crystal [10, 116], as well as the well-known ferroelectric compound (*S*)-(+)-*p*-(*n*-decyloxybenzylidene)-*p*-amino-(2-methylbutyl)cinnamate (DOBAMBC) [117]

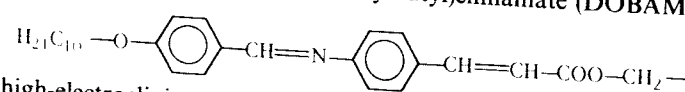

(15)

the high-electroclinic-coefficient substance W317 [118, 119]

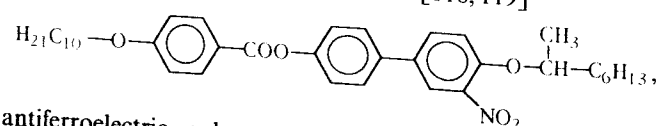

(16)

and the antiferroelectric substance (*R*)-4-(1-methylheptyloxycarbonyl)phenyl-4′-octyloxybiphenyl-4-carboxylate (MHPOBC) [120]

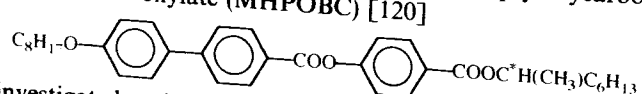

(17)

have been investigated so far.

Many systematic studies on preparation parameters for PDLCs and their influence on the electro-optic performance of displays have been made for NCAP systems by

Drzaic *et al.* [47–49, 121], for thermoplastic polymers by West *et al.* [62, 102], for thermally-cured epoxies by Doane *et al.* [5, 6], and Smith *et al.* [71, 122–123], for UV-cured systems by Vaz, Smith and Montgomery [75, 85, 93], Lackner, Margerum *et al.* [16, 77–79], and Coates, Nolan *et al.* [88–90, 112]. An important parameter for the electro-optic properties is the drop size which decreases with increasing phase separation speed (see figure 3). Both the threshold voltage and the switching speed of the resulting display decrease with increasing drop size (see figure 4), as discussed in the following section. The kinetics of the phase separation and thus the drop size can be

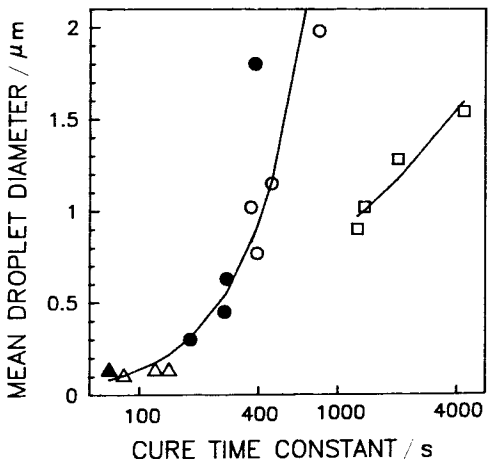

Figure 3. Drop size versus curing time for epoxy-based samples produced by PIPS. The cure rate was varied by changing the cure temperature and the accelerator concentration. For this particular system, two different mechanisms of droplet formation have been detected for $T = 325$ K and $T > 325$ K. From [122]. T_{cure}: ○, 350 K; ●, 362·5 K; △, 375 K; ▲, 387·5 K; □, 325 K.

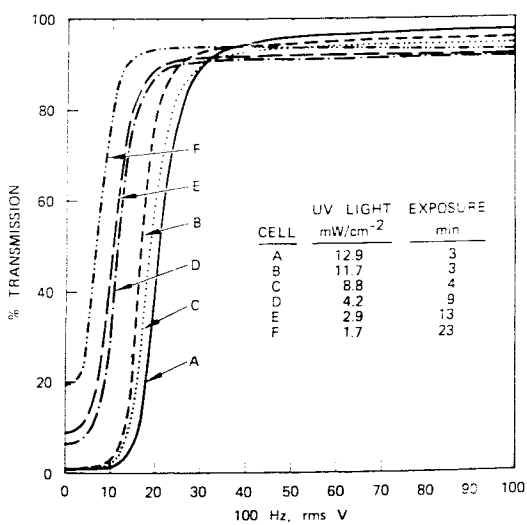

Figure 4. Optical transmission versus voltage for PDLC samples made using various UV intensity exposures. From [78].

controlled by the temperature and the addition of accelerators (PIPS, thermal curing), by the UV-intensity (PIPS, photopolymerization), by the cooling rate (TIPS) and by the rate of evaporation (SIPS). Using calorimetry in conjunction with scanning electron microscopy [71, 75, 85, 122, 123], the results of the phase separation have been systematically studied for particular systems. The phase separation kinetics can be investigated by time resolved measurements of the refractive index [57] or of the resistivity [124], and by determination of the structure factor using light scattering [125].

3. Nematic PDLCs

3.1. *Application*

Nematic PDLC films show some major advantages compared to conventional cells [7]: (1) No surface stabilization by glass substrates and thus *no complicated surface treatment* is required. (2) Since no glass plates are necessary, large area *flexible* light shutters can be produced. (3) Nematic PDLC displays work without polarizers and thus have a *high transmission* in the clear ON state (see figure 4). These convenient properties have been used to develop transmissive displays [7, 8], privacy windows [44, 126], and projection displays [63, 127, 128] (see figure 2 (*a*)). The reflective display shown in figure 2 (*b*) is equipped with a coloured reflector; the liquid crystal is doped with a dichroic dye to enhance the contrast [48]. Such reflective displays can be used to display the state of touch switches underneath the PDLC film.

For fail safe devices, *reverse-mode* displays have been developed which appear transparent in the OFF state and opaque in the ON state [113, 84]. These devices require a uniform alignment in the field-off state and make use of the electric field-induced disalignment of the director in materials with negative dielectric anisotropy (see figure 1 (*c*)). Besides these common applications, the use of PDLC devices as *IR shutters* has been suggested [15, 101], or the use of the mismatching of the refractive indices in PDLC films with $n_p > n_o$ for *angular discriminating filters* [60]. Films incorporating a dual-frequency addressable liquid crystal may work as *thermoelectro-optic switches* [94], due to the temperature dependence of the relaxation frequency where the sign of ε_a is reversed. Special systems which show only partial relaxation may be used as *memories* [100, 82]. The shear-induced surface alignment of droplets prepared in a SIPS process and its effect on the electro-optic properties has been proposed for use in *gas flow sensors* [103]. Optically induced *cis–trans*-transitions in stilbene-doped PDLCs [55] can affect the director field inside the drops and may be utilized for *optical sensors*. UV-curable adhesives are perfectly suitable for *in situ* induction of spatially periodic structures during photopolymerization; the resulting PDLC films provide *optical gratings* [78] or *Fresnel zone lenses* [129]. *Non-linear optical effects* [57, 130] have been observed in dye-doped systems. In addition, surface-induced *second harmonic generation*, and modulation of the SHG signal by a DC electric field has been demonstrated [131].

For normal display applications, high contrast and high on-state clarity, low threshold voltages, and fast switching times are desirable. These properties are affected by the refractive indices of the liquid crystal (n_e, n_o) and the polymer (n_p), the film thickness d (typically $\approx 20\,\mu m$), the droplet radius R (typically $\approx 1\,\mu m$) and shape, the director configuration, the viscosity γ_1 of the liquid crystal and, to a considerable extent on shielding effects due to the dielectric and ionic conductivity of both the polymer and liquid crystal. For an isolated droplet in the polymer matrix, the relation between the local electric field strength E' and the external field E is approximately described (at low

frequencies) by $E' \approx 3E(\rho_p/\rho_{lc}+2)^{-1}$, where ρ_p and ρ_{lc} are the resistivities of the polymer and the liquid crystal [64]. With respect to theoretical models for the director field variation within the droplets, the reorientation of the bipolar structure (see figure 1 (*a*)) and the radial–axial transition (see figure 1 (*b*)) have been most extensively studied. For the latter effect, the electric coherence length $\xi = E^{-1}(K/\varepsilon_0\varepsilon_a)^{1/2}$ needs to become sufficiently small with respect to the extrapolation length $d_e = K/W_0$ (which is inversely proportional to the anchoring energy W_0); the transition occurs at $d_e/\xi \approx 0{\cdot}078$ [74]. However, the critical field resulting from this relation cannot simply be reduced by lowering the anchoring energy, since the existence of the radial director field in a droplet at $E=0$ requires a sufficiently high anchoring strength, i.e. the ratio R/d_e must exceed a certain value. These competing influences result in a threshold voltage for the radial–axial transition of approximately [5, 74]

$$V_R \approx d/3(\rho_p/\rho_{lc}+2)E' \approx d/R(\rho_p/\rho_{lc}+2)(K/\varepsilon_0\varepsilon_a)^{1/2}, \tag{1}$$

where K is an average of the elastic coefficients. For typical cell parameters ($K \approx 10$ pN, $\varepsilon_a \approx 12$, $\rho_p/\rho_{lc} \approx 10$), V_R is very high ($V_R \approx 60$ V). Considerably smaller voltages (≈ 20 V and less) can be obtained for bipolar droplets [6]

$$V_B = 2d/3a(\rho_p/\rho_{lc}+2)[K(L^2-1)/\varepsilon_0\varepsilon_a]^{1/2}. \tag{2}$$

The latter voltage depends on the aspect ratio $L = a/b$ between the major axis a and the minor axis b of the elliptical droplets. The high switching voltages of PDLCs can be reduced to a few volts [63, 86, 132], provided that the conductivity of the liquid crystal is sufficiently small (or the conductivity of the polymer is large) [133]. Thus, active matrix technologies could be applied to produce spatial light modulators as presented in figure 2 (*a*). With respect to the curing rates—and thus the droplet size—a trade-off has to be made, since large drop sizes provide low switching voltages (see figure 4) whereas small droplet sizes result in higher switching speed and better contrast.

For bipolar droplets, the elliptical shape is essential, not only for the switching voltage, but also for the relaxation times [64]

$$\tau_{off} = \gamma_1 a^2/K(L^2-1), \tag{3}$$

which can be considerably reduced, depending on the aspect ratio L of the droplets (see figure 5 (*a*)). The respective rise time is again dominated by the ratio ρ_p/ρ_{lc} [64]. In *dyed* NCAP systems, a two step mechanism was observed (see figure 5 (*b*)) with characteristic time constants of $\tau_{1,on} = 1$ ms, $\tau_{2,on} \approx 100$ ms and $\tau_{1,off} < 10$ ms, $\tau_{2,off} \approx 100$ ms, respectively [45].

The contrast ratio measured with a collimated light beam at normal light incidence and a small acceptance angle of the detector can be up to 200 : 1 [58, 132]. However, since the electro-optic effect is due to scattering, lower values may be obtained for different illumination conditions and high acceptance angles of the detector [77]. The transmission in the opaque state depends on the film thickness, the volume density of the droplets and the total scattering cross section of a droplet, which has been theoretically calculated for various director configurations [134–135]; most recently, multiple scattering effects have been considered [91]. For minimum transmission, the drop size and spacing should be of the order of the wavelength of light. The transmission in the transparent state depends mainly on the index matching between n_o and n_p. To avoid mismatching for non-normal observation, *haze-free* light shutters have been proposed which consist of liquid crystal droplets embedded in a homeotropically aligned liquid crystal polymer [68, 69]. In this case, both the ordinary and the

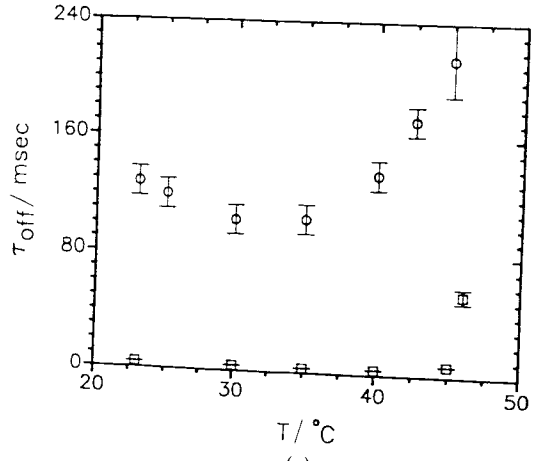

(*a*)

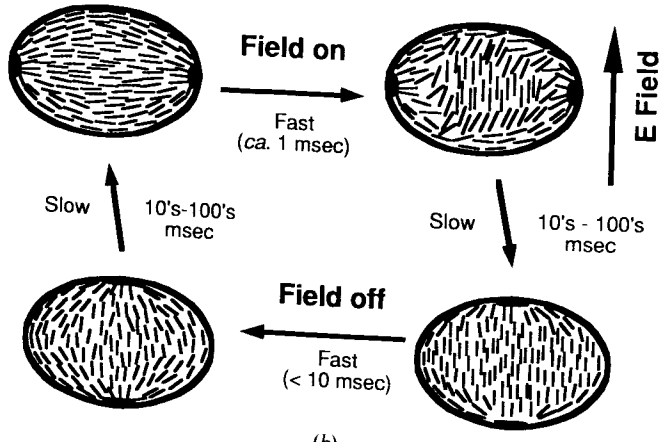

(*b*)

Figure 5. (*a*) Relaxation time τ_{off} versus temperature for spherical (○) and elliptical (□) bipolar droplets (from [64]). (*b*) Model for the two-stage rise time and decay time response of bipolar droplets in NCAP films. From [45].

extraordinary refractive index of the monomer can be matched with the respective refractive indices of the matrix, thereby increasing the angular width of the transmission considerably (see figure 6). A different approach to realize haze-free displays is the use of anisotropic gels which contain a large fraction of liquid crystal which is stabilized by a small amount of cross-linked mesogenic network. In nematic gel displays, the refractive index matching (in the field-off state) or mismatching (in the field-on state) between the monomer and the polymer is used [104], while the more recently invented cholesteric gel displays [108] provide switching between the transparent Grandjean texture (planar alignment) and the diffuse scattering focal-conic texture of the cholesteric phase. In the latter case, the only effect of the polymer is to stabilize the texture appearing in the field-off state.

The contrast of PDLC light shutters can be enhanced using the *guest-host effect* [136], by incorporating a pleochroic dye in NCAP droplets [7]. This effect is used in the reflective PDLC display represented in figure 2(*b*) [48, 53, 121]: here a coloured

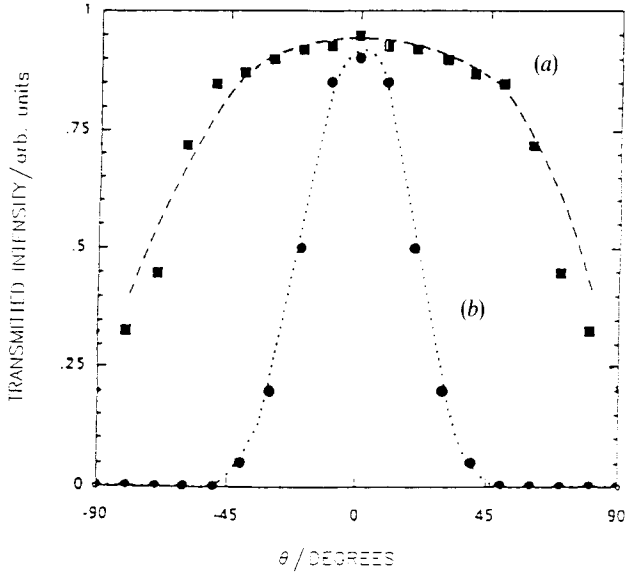

Figure 6. Angular dependence of transmitted light for: (*a*), a wide angle view shutter (polymer liquid crystal matrix) and (*b*), a normal PDLC shutter (isotropic polymer matrix). From [68].

reflector provides high brightness in the ON state, while absorption by the dye in the OFF state decreases the reflectivity, in addition to the scattering effect. Even without dichroism, the contrast can be improved by embedding an *isotropic dye* in a PDLC film [65]. In the transparent state, the optical path length corresponds to the cell thickness; in the opaque state it is much longer due to multiple scattering, and according to the Lambert–Beer law, the transmittance decreases exponentially.

3.2. *Structure of nematic micro-droplets*

While the most stable structure of the bulk nematic phase is given by a uniform orientation of the director, the confinement of nematic liquid crystals to spherical cavities can lead to a variety of quite complicated director fields (see figure 7). The occurrence of the different structures depends on the anchoring of the director at the droplet surface, on the size of the droplet, on the elastic properties of the liquid crystal, and on external fields. For planar anchoring, bipolar [137], twisted bipolar [25, 138–140], and concentric [37] (=toroidal [138]) structures are most commonly observed, while homeotropic boundary conditions cause the appearance of radial [137, 141], twisted radial [34], and axial structures [137]. Escaped twisted radial and twisted axial structures have been observed in electric fields [142]. All of these droplet structures exhibit defects, i.e. points or lines where the director is not defined. The radial structure shows a hedgehog defect, i.e. a volume defect with the topological charge $N = 1$; the bipolar structure is characterized by two surface point defects, boojums [143]. The toroidal structure contains a diametrical line defect with strength $s = 1$; the axial structure requires an equatorial line defect with $s = 1/2$. The classification of defects in nematic droplets and the topological aspects of the transformation between surface and volume defects have been extensively discussed by Volovik and Lavrentovich *et al.* [30, 39, 144].

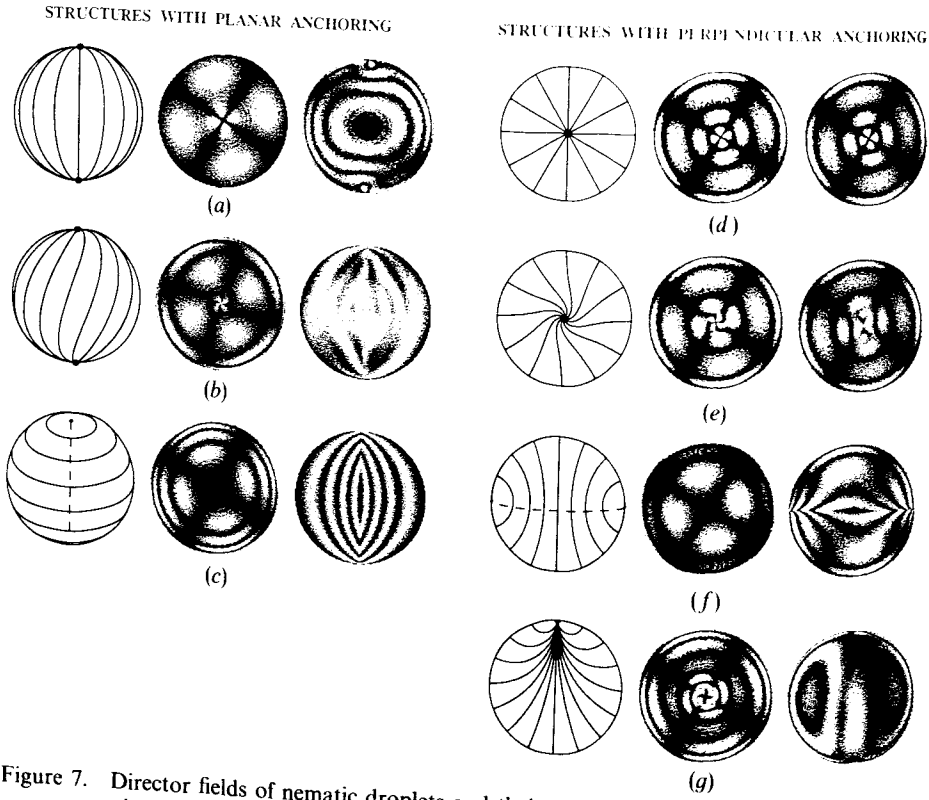

Figure 7. Director fields of nematic droplets and their appearance in transmission between crossed polarizers (drop radius $R = 12\,\mu m$, $n_o = 1{\cdot}5$, $n_e = 1{\cdot}6$). For planar boundary conditions (*a–c*), the director field on a spherical shell is presented, while for perpendicular anchoring (*d–g*), planar sections of the director field are shown. The respective transmission intensities were calculated for observation parallel and perpendicular to the polar axis of the director field and corresponds to azimuthal orientations of the polarizer (analyser) of 60° (−30°). (*a*) Bipolar, (*b*) twisted bipolar, (*c*) toroidal or concentric, (*d*) radial, (*e*) twisted radial, (*f*) axial, and (*g*) escaped twisted radial structure.

For given boundary conditions, the resulting structure is determined by the competing influences of elastic forces and external fields. For a liquid crystal with positive dielectric anisotropy ε_a, in an electric field E, the free energy is given by

$$F = \frac{1}{2}\int [K_{11}(\operatorname{div}\mathbf{d})^2 + K_{22}(\mathbf{d}\cdot\operatorname{rot}\mathbf{d})^2 + K_{33}(\mathbf{d}\times\operatorname{rot}\mathbf{d})^2 + K_{13}\operatorname{div}(\mathbf{d}\operatorname{div}\mathbf{d}) - K_{24}\operatorname{div}(\mathbf{d}\times\operatorname{rot}\mathbf{d} + \mathbf{d}\operatorname{div}\mathbf{d})]\,dV - \frac{1}{2}\int \varepsilon_0\varepsilon_a(\mathbf{E}\cdot\mathbf{d})^2\,dV + \frac{1}{2}\int W_0 \sin^2\phi\,dA. \quad (4)$$

The first three terms in equation (4) correspond to the usual Frank free energy for elastic deformations of the director field $\mathbf{d}(\mathbf{r})$, with K_{11}, K_{22}, and K_{33} being the elastic constants for splay, twist, and bend deformation, respectively. In contrast to liquid crystals in the bulk, the splay-bend term (with the coefficient K_{13}) and saddle-splay term (with the coefficient K_{24}) have to be considered as well. Using Gauss's theorem,

the volume integrals of the latter terms can be converted to surface integrals and thus vanish for liquid crystals in the bulk. The last term in equation (4) corresponds to the anchoring of the director at the surface and depends on the anchoring energy W_0 and on the angle ϕ between the actual director and its most stable orientation. Typical values for the coefficients in equation (4) are $K_{ii} \approx 5 \times 10^{-12}$ N [73], $-6 \leqslant \varepsilon_a \leqslant 12$, and $W_0 = 10^{-5}$–10^{-4} Jm^{-2} [18, 74]. Due to the surface effects which dominate liquid crystals in small cavities, the saddle splay constant K_{24} has been determined for the first time by means of NMR measurements [18]. A ratio of $K_{24}/K = 1 \pm 0{\cdot}6$ was found from the experimental data, assuming an equal-constants approximation: $K_{11} = K_{22} = K_{33} = K$.

Although most theoretical considerations use this equal-constants approximation, the bend to splay ratio varies in usual nematic liquid crystals between $K_{33}/K_{11} \approx 0{\cdot}7$ and $K_{33}/K_{11} \approx 2$ [37] and can be even larger close to a nematic–smectic phase transition [144]. Thus, the occurrence of the different structures depends not only on the anchoring conditions and on the droplet size, but is also affected by this ratio. In a particular system with planar boundary conditions, the toroidal structure (which exhibits only bend deformation) was found to occur for $K_{33}/K_{11} < 0{\cdot}95$, whereas the bipolar structure is stable for larger values of this ratio [37]. A transition from the bipolar to the twisted bipolar structure is expected to occur when $K_{11} \geqslant K_{22} + 0{\cdot}431$ K_{33} [138], i.e. even for non-chiral liquid crystals, the elastic energy is reduced by the occurrence of twist, if the splay constant is relatively large. In the case of perpendicular anchoring, the radial configuration (pure splay) is stable for large values of K_{33}/K_{11}, while the axial configuration (splay and bend) occurs for small values of this ratio. A twisted hyperbolic structure [144] was predicted to be more stable than the radial configuration, unless the bend to splay ratio is unusually large, $K_{33}/K_{11} > 6$; however the stability of the twisted hyperbolic model with respect to the more recently identified twisted radial structure [142] has not been proved yet.

Due to its importance for electro-optic applications, the radial–axial transition has been very extensively studied both theoretically [20, 73, 137, 145 146] and experimentally [34, 42, 73, 147]. Free energy calculations and experiments confirm that the axial configuration is more stable for small ratios R/d_e between the drop radius and the surface extrapolation length $d_e = K/W_0$, and that the axial structure is stabilized by electric fields for $\varepsilon_a > 0$. In addition to these very reasonable results, an interesting reentrant phenomenon has been discovered: for constant field strength the axial structure occurs for very small and very large diameters of the droplet, while the radial structure is stable for medium diameters [73]. In agreement with the theoretical prediction of a triple point [145], an intermediate state between the radial and the axial structure was also observed in electric fields [42]. This structure shows an $s = 1$ 2 ring defect with a diameter smaller than the droplet diameter. The appearance of such a structure is in agreement with Monte Carlo simulations [148] and with recent computer simulations [149] based on a relaxation equation for the alignment tensor [150].

In order to identify the different types of director fields, either deuterium NMR studies [70, 151–152] or—for sufficiently large drop sizes—observation using a polarizing microscope can be used (see figure 7). In the NMR technique, the dependence of the quadrupole splitting on the angle θ between the magnetic field and the local director is used, and the distribution of the different orientations θ (without spatial resolution) can be obtained from the spectral shape of the NMR lines. In contrast, optical investigation gives no quantitative values of the angular distribution

function, but contains detailed spatial information on the director field within a droplet. The comparison of microscopic pictures with calculated transmission patterns for given director fields is a surprisingly sensitive tool to get information on the structure. For such calculations, the Jones [95] or the Müller–Stokes formalism [142] has been used. To calculate the change of the polarization and intensity of a transmitted light beam, the droplet can be considered as consisting of thin slices of thickness h. Each slice introduces a phase shift

$$\delta = 2\pi(n_{e,\,\mathrm{eff}} - n_o)h/\lambda \tag{5}$$

between the two linearly polarized components parallel and perpendicular to the local director. The effective refractive index $n_{e,\,\mathrm{eff}}$ depends on the angle ϑ_d between the local director and the direction of light propagation:

$$n_{e,\,\mathrm{eff}} = [\sin^2 \vartheta_d/n_e^2 + \cos^2 \vartheta_d/n_o^2]^{-1/2}. \tag{6}$$

Successive multiplication of the Stokes vector (Jones vector) with the respective Müller matrices (Jones matrices) [153] leads to the intensity for a particular point of the orthoscopic picture. Figure 7 demonstrates the characteristic differences of the transmission for various structures.

4. Cholesteric PDLCs

4.1. *Principle of the cholesteric PDLC colour display*

Extending the work on nematic PDLCs to chiral liquid crystals, Crooker and Yang [9] have proposed reflective colour displays using polymer-dispersed cholesteric liquid crystals PDCLC. The cholesteric phase is locally nematic, but the director rotates spatially and exhibits a helical structure, characterized by its pitch p. Due to the spatial periodicity $p/2$ of the twisted director field, uniformly oriented samples with sufficiently short pitch show selective reflection of circularly polarized light at the Bragg wavelength

$$\lambda_0 = np, \tag{7}$$

where n is a mean value of the refractive indices. The electro-optic effect is based on the fact that a cholesteric droplet confined to a small spherical cavity exhibits no selective reflection, since anchoring of the director at the surface causes a non-uniform orientation of the pitch axis. However, for negative dielectric anisotropy of the liquid crystal, external electric fields favour a planar alignment of the director in the plane perpendicular to the field. Thus, an applied voltage may overcome the effect of the boundary conditions and induce a uniform orientation of the pitch axis along the field. As a consequence, the reflectivity increases with increasing field strength (see figure 8). The reflection colour, however, depends on the chirality of the material. In mixtures of a nematic compound and a chiral dopant, the pitch, and thus the wavelength λ_0, can be controlled by the concentration c of the chiral dopant, according to

$$p \cdot c = p_0, \tag{8}$$

where p_0 is a constant. This relation describes an ideal mixture and is valid for most cholesteric mixtures.

Similarly to the electro-optic characteristics of nematic PDLCs, the increase of the reflectivity with increasing voltage shows a small slope (see figure 8). Thus, the device is not suitable for multiplexing, but provides the advantage of controlling the reflectivity very accurately [9, 154]. Moreover, the spectral bandwidth is quite narrow (typically $\approx$ 40–50 nm) and thus the chromaticity coordinates are close to those of

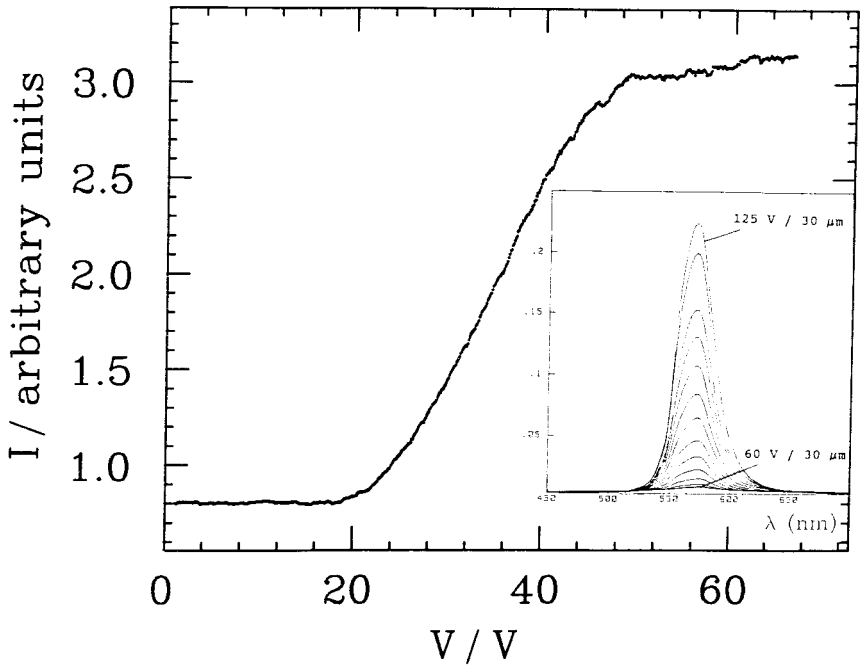

Figure 8. Reflectivity versus voltage for a PDCLC display ($d \approx 10\,\mu$m). Inset: selective reflection spectra for different voltages ($d = 30\,\mu$m). From [155].

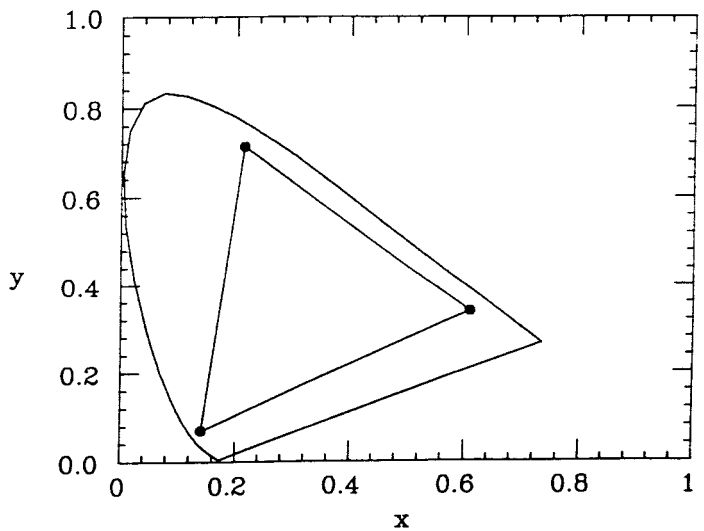

Figure 9. Chromaticity coordinates in the 1935 CIE convention for three PDCLC samples with different colours of the selective reflection due to different concentrations c of the chiral compound (CE2). $c = 22{\cdot}0$ per cent: blue, $(x, y) = (0{\cdot}141, 0{\cdot}070)$; $c = 19{\cdot}6$ per cent: green, $(x, y) = (0{\cdot}213, 0{\cdot}711)$; $c = 15{\cdot}1$ per cent: red, $(x, y) = (0{\cdot}609, 0{\cdot}338)$. From [155].

monochromatic light (see figure 9). As a consequence, a large area of the chromaticity diagram can be achieved by additive colour mixing, when reflective PDCLC sheets are stacked on top of each other [155]. However, even in the best case only one handedness of circularly polarized light, and thus not more than 50 per cent of the incident light, is reflected.

The intensity I of the selective reflection, the spectral width $\Delta\lambda$, and the angular width $\Delta\vartheta$ of the scattered light for normal light incidence depend on the droplet radius R [156] which, in turn, is determined by the speed of the phase separation [154]. The intensity is related to R according to $I \propto VR^3$, where V is the volume of the phase separated liquid crystal. The dependence of the spectral and the angular width on R can be approximately described by the uncertainty relation

$$|\mathbf{k}_0 - \mathbf{k}_{1/2}|R = 1{\cdot}81, \tag{9}$$

where $\mathbf{k}_0$ is the wavevector which satisfies the Bragg condition exactly, i.e. the scattered intensity I shows a maximum value I_0; $\mathbf{k}_{1/2}$ is the wavevector corresponding to $I = I_0/2$. According to equation (9), both $\Delta\lambda$ and $\Delta\vartheta$ are inversely proportional to R [156].

The switching times reported for systems prepared by TIPS are not below 100 ms [9, 157], but the speed has been improved using UV-cured polymers to time constants of a few ms [156]. Moreover, the samples prepared by PIPS are suitable for operation at room temperature [9, 156].

4.2. *Structure of cholesteric droplets*

If the helical pitch is a few μm or larger, the structure of the director field in cholesteric droplets can be easily studied using a polarizing microscope. In this case, fingerprint lines can be seen (see figure 10(*a*)). The distance of these lines is approximately $p/2$, and thus the simple observation of cholesteric droplets dispersed in a viscous fluid (for example, glycerol) can be used to measure the pitch p and to determine the handedness of the helix [158]. Depending on the orientation of the droplet, the fingerprint lines usually form a spiral or concentric rings (see figure 10(*b*)), indicating that the pitch axes are arranged in a radial fashion [36, 159–161]. The director field of such droplets can be described [162] by

$$\mathbf{d} = \mathbf{e}_\phi \cos\Omega + \mathbf{e}_\vartheta \sin\Omega, \tag{10}$$

where $\mathbf{e}_\phi$ and $\mathbf{e}_\vartheta$ are unit vectors along the azimuthal and the polar direction in spherical polar coordinates, and

$$\Omega = (s-1)\phi + \Omega_0 + \mathbf{q}\cdot\mathbf{r} \tag{11}$$

describes the orientation of the director parallel to a spherical surface with radius $|\mathbf{r}|$. As proposed by Frank and Pryce [160], the radial disclination line occurring in the droplets represented in figure 10(*b*) is characterized by the strength $s = 2$. However, cholesteric droplets with a diametrical $s = 1$ disclination line have also been observed for some materials [36]. The stability of these topologically different director fields for droplets with planar anchoring conditions has been extensively discussed by Bezić and Žumer [162].

In magnetic [34, 163] or transverse electric [164] fields, the observed concentric rings of Frank–Pryce droplets with positive magnetic or dielectric anisotropy become ellipse-like with their long axes along the field direction (see figure 10(*d*)). This behaviour is consistent with a reorientation of the director along the field direction, and thus a reorientation of the helical axis perpendicular to the field. Observations of cholesteric droplets along the field direction [163, 164] indicate helical unwinding, i.e. an increase of the pitch with increasing field strength, as known for cholesteric liquid

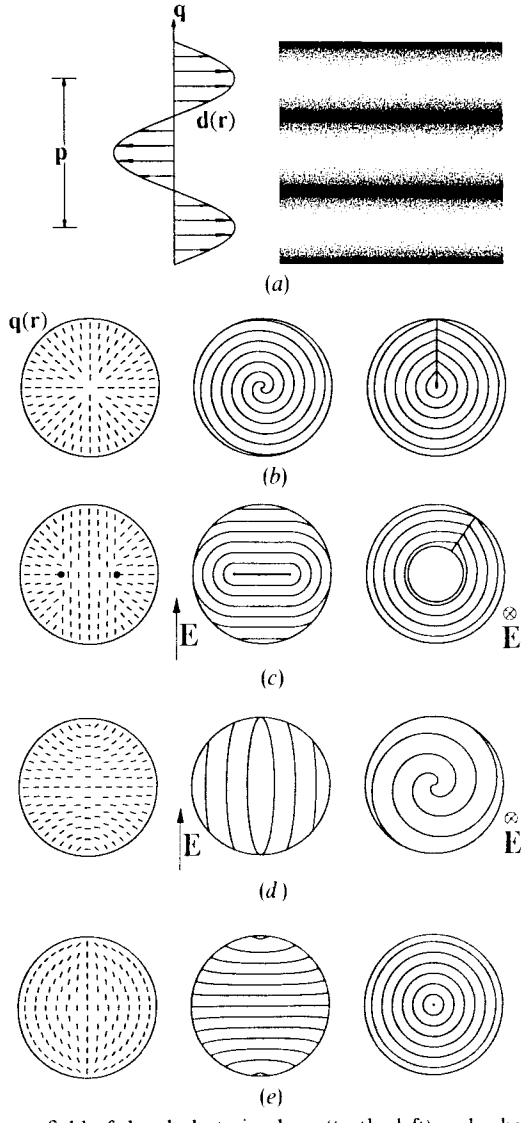

Figure 10. (*a*) Director field of the cholesteric phase (to the left) and schematic presentation of the fingerprint lines (to the right). (*b–e*) **q**-fields of cholesteric droplets and their fingerprint patterns as observed by microscopy: (*b*) spherulite structure (Frank–Pryce model, planar anchoring), (*c*) droplet with $\varepsilon_a < 0$ in an electric field, (*d*) droplet with $\varepsilon_a > 0$ in an electric field, (*e*) cholesteric droplet with perpendicular anchoring.

crystals in the bulk [165]. More interesting, and relevant to the electro-optic PDLC application proposed by Crooker and Yang, is the investigation of large pitch droplets with negative dielectric anisotropy in electric fields [166]. The study of the latter systems indicates the appearance of a region with uniform orientation of the pitch axis in the centre of each droplet (see figure 10(*c*)) [166, 167]. Additional observations in transverse fields indicate that this reorientation is connected to the appearance of a disclination *ring* in the plane perpendicular to the field [164]. The continuous increase of the reflectivity in droplets with small pitch corresponds to an increase of the diameter

ρ of the disclination ring with increasing field strength. Both the threshold voltage for the appearance of the disclination ring and the slope $d\rho/dE$ were found to decrease with increasing pitch and with increasing droplet diameter, respectively [167]. Finally, for very high field strength, the director field approaches an 'aligned' texture [168], which is characterized by a uniform alignment of the pitch axis along the field direction, a bipolar director field (with varying azimuthal angle) in the planes perpendicular to the field, and a spiral disclination line at the surface [166, 168 169].

Although the Frank–Pryce model is characterized by planar boundary conditions, the respective pattern (see figure 10(*b*)) is also stable in matrices which are known to provide homeotropic anchoring for nematic liquid crystals [168]. Only recently, a different type of droplet has been observed in PIBMA [164] or in NOA-65 at elevated temperatures [92]: the occurrence of either concentric rings or parallel lines in the fingerprint pattern (see figure 10(*e*)) indicates a bipolar structure of the **q** field which is consistent with perpendicular anchoring of the director [164]. The behaviour of this type of droplet in electric fields has still to be investigated.

5. Ferroelectric and antiferroelectric PDLCs

Ferroelectric liquid crystals are known for very fast switching electro-optic effects [11]: switching times of about 1 μs or even less are not unusual. Thus, efforts have also been made to use these liquid crystals for PDLC devices. In recent work, two types of PDFLC (polymer-dispersed ferroelectric liquid crystal) displays have been proposed. One possibility is to use the liquid crystal as a wave plate with tunable optical axis and place it between crossed polarizers [10]. This method is based on the same principles as conventional devices such as the surface stabilized ferroelectric liquid crystal display [170] where a thin film of liquid crystal is contained between ITO-coated glass plates. The second method of operation [117] is based on refractive index matching or mismatching between the liquid crystal and the polymer, similar to nematic PDLC displays. Recently, *volume-stabilized ferroelectric liquid crystal displays* [17] have also been proposed, where the orientation of the liquid crystal in a conventional cell is stabilized by the addition of a cross-linked polymer network.

5.1. *Conventional applications of ferroelectric liquid crystals*

A variety of electro-optic effects can be used for applications utilizing ferroelectric liquid crystals. Ferroelectric properties occur in chiral smectic liquid crystals which—in addition to the orientational order of the molecules—exhibit a layer structure [171]. If the tilt angle θ between the director **d** and the layer normal $\mathbf{q}_l$ is non-zero and if the molecules are chiral, a spontaneous polarization $\mathbf{P}_s$ may occur along the two-fold symmetry axis of the structure which is perpendicular to both **d** and $\mathbf{q}_l$, i.e. $\mathbf{P}_s = P_0 \mathbf{q}_l \times \mathbf{d}$ [172]. Despite the local appearance of $\mathbf{P}_s$, the macroscopic value of the spontaneous polarization for a tilted chiral smectic phase, for example S_C^*, is usually zero in the field-off state, because these phases form a helical structure. However, the coupling of $\mathbf{P}_s$ to an external electric field can cause a field-induced *helical unwinding* [173] (see figure 11(*a*)). Moreover, *bistable switching* (see figure 11(*b*)) can be achieved in the SSFLCD (surface-stabilized ferroelectric liquid crystal display) [170] where the helical structure in a very thin liquid crystal film is suppressed by surface anchoring at the glass substrates. Coupling between θ and $\mathbf{P}_s$ causes the electroclinic effect [174], for example, the field-induced appearance of a tilt angle in non-tilted chiral smectic structures such as the S_A^* phase (see figure 11(*c*)). Finally, antiferroelectric phases such as $S_{C_A}^*$ [175] (where the tilt direction and thus the sign of $\mathbf{P}_s$ alternate from layer to layer) provide the

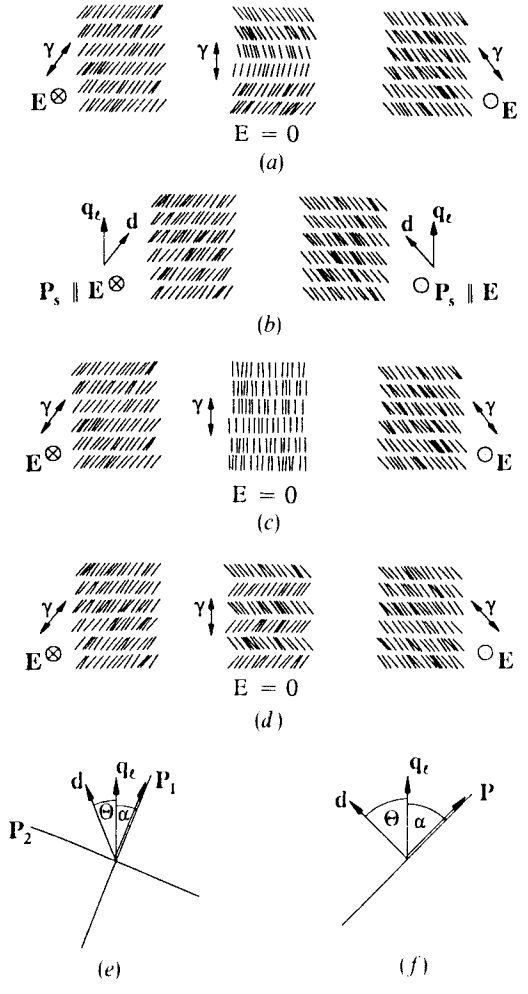

Figure 11. (*a–d*) Director fields for different switching effects in ferroelectric liquid crystals (γ: optical axis, $\mathbf{q}_l$: layer normal, **d**: director, $\mathbf{P}_s$: spontaneous polarization. (*a*) Helical unwinding, (*b*) bistable switching in surface-stabilized FLC displays, (*c*) electroclinic effect, (*d*) tri-stable switching in antiferroelectric liquid crystals. (*e–f*) azimuthal orientation of the layer normal $\mathbf{q}_l$ with respect to the polarizer $\mathbf{P}_1$ and analyser $\mathbf{P}_2$, in order to maximize the contrast when (*e*) the optical retardation of the PDLC film, or (*f*) the scattering effect due to matching or mismatching of the refractive indices is used.

possibility of tri-stable switching due to a discontinuous antiferroelectric–ferroelectric transition (see figure 11 (*d*)). For all of these electrooptic applications, the liquid crystal film is placed between crossed polarizers and used as an optical retarder. The main effect of the electric field is to rotate the optical axis around the field direction, thereby causing a variation of the transmittance. The intensity of the transmitted light is given by

$$I(\psi) = \tfrac{1}{2} I_0 \sin^2 2\psi \sin^2 \tfrac{1}{2}\delta, \tag{12}$$

where δ is the retardation; ψ is the azimuthal angle between the optical axis γ of the liquid crystal and the polarization plane of the incident light.

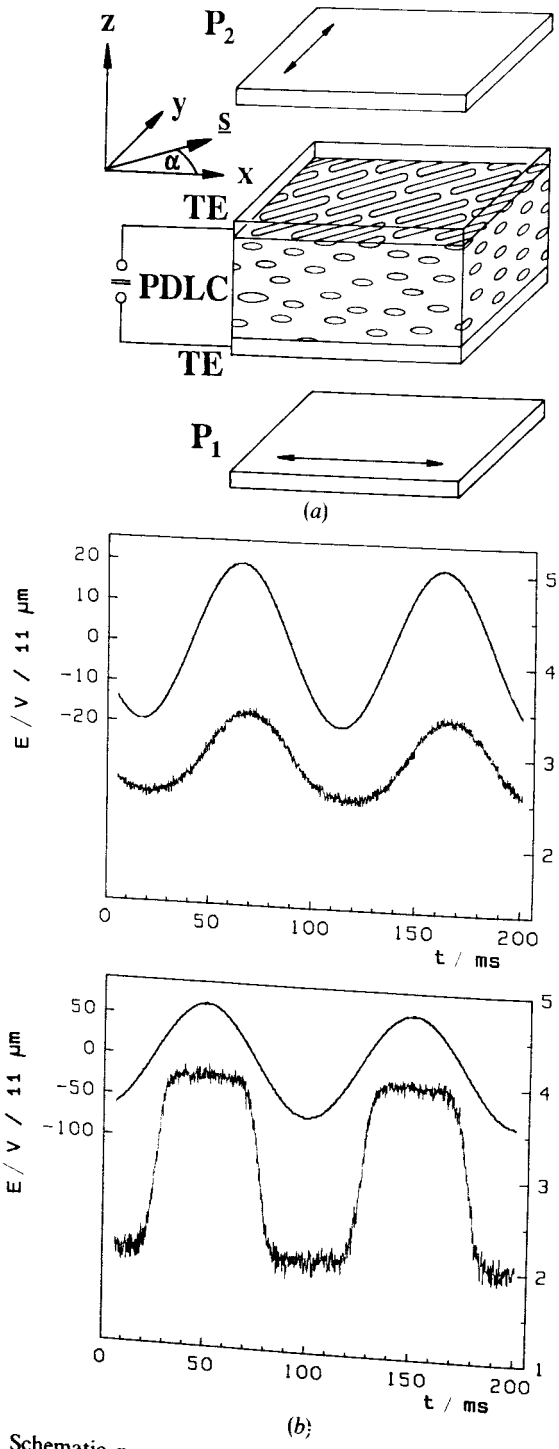

Figure 12. (*a*) Schematic presentation of the ferroelectric PDLC display TE, transparent electrode layers; P_1, P_2, polarizers; s, shear direction of the PDLC film. From [10]. (*b*) Electro-optic response due to helical unwinding for low and high voltages. From [116].

5.2. *Helical unwinding in PDFLCs*

By means of UV-curable adhesives, prealigned smectic samples can be obtained by shear flow during the polymerization-induced phase separation [10]. For this purpose, the homogeneous mixture of the liquid crystal and the polymer precursor is sandwiched between ITO- coated glass slides and these slides are gently sheared during the exposure of the sample to UV light. Electro-optic switching at room temperature has been demonstrated using a liquid crystal mixture consisting of 20 per cent (by weight) of the chiral compound (**14**) and 80 per cent of the non-chiral smectic component 5-octyl-2-[4-octyloxyphenyl]pyrimidine. Mixing this liquid crystal with Norland Optical Adhesive NOA-65, curing with an irradiance of $\approx 12\,\mathrm{mWcm}^{-2}$, and shearing during the exposure has resulted in birefringent PDLC films with elliptical droplets. For sufficiently large droplets, parallel dark and bright lines perpendicular to the shear direction have been observed by polarizing microscopy [116], which is typical for a uniformly oriented helical structure [176] of the S_C^* phase. Due to helical unwinding [173], the optical axis γ of these samples (which is parallel to the shear direction **s** in the field-OFF state) is rotated under the influence of electric fields. In contrast to nematic and cholesteric PDLC devices, the sample has to be placed between crossed polarizers for electro-optic applications (see figure 12 (*a*)). The electro-optical response depends considerably on the azimuthal angle α between the shear direction and the plane of polarization of the incident light. According to equation (12), switching between two azimuthal orientations of the optical axis, $\psi_1 = \alpha + \theta$ and $\psi_2 = \alpha - \theta$, results in a change of the transmitted intensity

$$\Delta I(\alpha, \theta) = \tfrac{1}{2} I_0 \sin^2 \tfrac{1}{2}\delta \sin 4\alpha \sin 4\theta. \tag{13}$$

Thus, maximum contrast is obtained for a retardance of $\delta = \pi$ (half-wave plate), an azimuthal angle of $\alpha = 22{\cdot}5^\circ$ between the shear direction of the PDLC film and the plane of polarization, and a tilt angle of $\theta = 22{\cdot}5^\circ$ (see figure 11 (*e*)). In this set-up (see figure 12 (*a*)), linear electro-optic modulation is possible for small fields, while saturation occurs for complete unwinding of the helix (see figure 12 (*b*)). The spontaneous polarization, measured by the triangular wave method [177] shows a temperature dependence which is typical for the S_C^* phase (figure 13). The switching

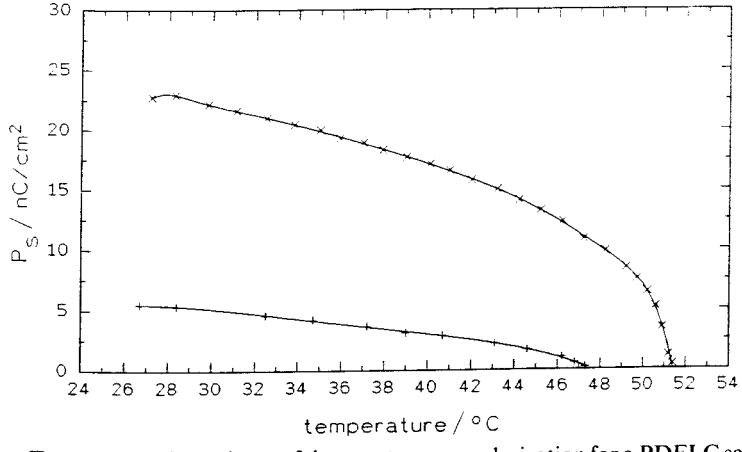

Figure 13. Temperature dependence of the spontaneous polarization for a PDFLC sample (+) and the respective monomer liquid crystal (×). From [116].

times decrease with increasing field strength and values of a few hundred μs have been found for sufficiently high fields [10, 116]. The values of τ are still two orders of magnitude higher than the switching times of the pure monomer, while the values of $\mathbf{P}_s$ and the phase transition temperatures were slightly lower than expected. This indicates that the phase separation in samples investigated so far was incomplete, and thus it is expected that the electro-optic properties can be considerably improved. More recent systematic investigations [178] show that *bistable* switching can be obtained for high UV intensities during the preparation, i.e. for small cavity sizes within the polymer film.

5.3. *Electroclinic effects in PDFLCs*

Owing to coupling of the tilt angle θ to an applied field E, electro-optic switching can also occur in the S_A^* phase or other non-tilted smectic phases. Depending on the electroclinic coefficient e_c, a tilt angle

$$\theta = e_c E \tag{14}$$

is induced by electric fields in these phases. In PDLC samples consisting of the pure compound (**14**) and the polymer formed by NOA-65, this electroclinic effect has been observed in the S_A^* temperature range between 68·6 and 74·4°C (see figure 14) [10, 115]. As for the investigation of helical unwinding, the samples were sheared during the photopolymerization in order to get a uniform orientation of the smectic layer normal. Again, the electro-optic effect is because of the rotation of the optical axis around the field direction, and according to equations (12) and (14), a linear relation between the transmittance and the applied field is obtained if the polarizer and analyser are adjusted to $\alpha = 22{\cdot}5$ and $112{\cdot}5°$ and the induced tilt angle is small. In agreement with the theoretical prediction $e_c \propto (T - T_c)^{-1}$, the electroclinic coefficient increases with decreasing temperature, thereby varying from 2·1 to $0{\cdot}5 \times 10^{-3}$ rad·μm V^{-1}. Close to the transition to the S_C^* phase, the dependence $\theta(E)$ becomes non-linear due to pretransitional behaviour. In contrast to the effect of helical unwinding, the switching times $\tau = \gamma_0 \alpha^{-1}(T - T_c)^{-1}$ for the electroclinic effect depend only on the temperature T and the tilt viscosity γ_0, but not on the applied field strength. The values of the electroclinic switching times have been found to be about $\tau = 100$–$200\ \mu$s.

The electroclinic effect has also been observed in samples prepared by temperature-induced phase separation using the ferroelectric liquid crystal W317 and the thermoplastic matrix poly(vinylbutyral) [119]. Komitov *et al.* [119], have obtained a

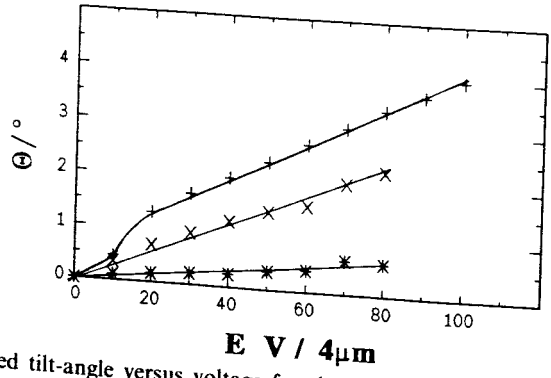

Figure 14. Induced tilt-angle versus voltage for the electroclinic effect in a PDLC sample containing the ferroelectric liquid crystal (14). From [10]. (+), 69°C; (×), 70°C; (*), 73°C.

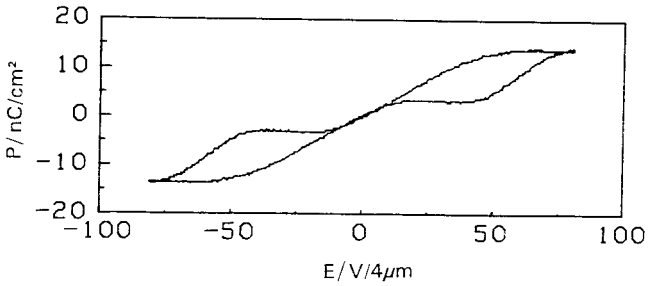

Figure 15. Hysteresis loop for an antiferroelectric PDLC sample containing MHPOBC. From [120].

prealignment of the liquid crystal by stretching the PDFLC film. A very large electroclinic coefficient $e_c \approx 8{\cdot}7 \times 10^{-3}$ rad·μm V^{-1} and switching times down to 128 μs (for 60 V_{pp}) have been found in their PDFLC films prepared by TIPS.

5.4. *Antiferroelectric switching in PDFLCs*

One of the most interesting topics in recent investigations on smectic liquid crystals is the discovery of various smectic phases showing a herringbone structure, i.e. an alternating tilt direction in neighbouring smectic layers. For the respective chiral smectic phase, an antiparallel order of the local spontaneous polarization occurs, resulting in *antiferroelectric* phases with vanishing total spontaneous polarization. In surface-stabilized cells, these phases show tristable switching due to field-induced phase transitions to the unwound ferroelectric state. The first and most thoroughly investigated compound which shows an antiferroelectric $S^*_{C_A}$ phase in the temperature range below the ferroelectric S^*_C phase is MHPOBC [175]. Using this liquid crystal, characteristic tristable switching behaviour was also found in PDLC films [120]. Although the hysteresis loop (see figure 15) is not perfect and the contrast ratios (about 3 : 1) are rather poor, it is remarkable that a PDLC film can give partial bistability (in the S^*_C phase) and tristability (in the $S^*_{C_A}$ phase) at all. This behaviour indicates that in sheared thin PDLC films, the helical structure can be—at least partially—unwound, as in a surface stabilized display, without any treatment of the glass plates covering the sample. Thus it seems worth trying both to analyse the mechanism for the flow-induced prealignment in more detail and to improve its quality.

5.5. *Scattering effects in PDFLCs*

Concurrent with the development of PDFLC films using the optical retardation of the liquid crystal, Zyryanov *et al.* [117], have created a scattering PDLC display using the ferroelectric liquid crystal DOBAMBC. As in nematic PDLC films, the ordinary refractive index of the liquid crystal is matched to the refractive index of the polymer. However, since the director stays in the film plane during its field-induced reorientation, *one polarizer* is necessary to get a contrast (see figure 11(*f*)). Maximum transmittance $T_\perp$ is achieved when the director is oriented perpendicular to the plane of polarization ($n_{eff} = n_o = n_p$), whereas the transmittance reaches a minimum value $T_\parallel$ due to scattering when the director is parallel to the polarization of the incident light ($n_{eff} = n_e \neq n_p$). As in the case of the PDFLC films described above, a uniform prealignment of the smectic droplets is essential. The transmitted intensity is given by

$$I(\psi) = \tfrac{1}{2} I_0 (T_\perp \sin^2 \psi + T_\parallel \cos^2 \psi), \tag{15}$$

where ψ is the azimuthal angle of the optical axis with respect to the polarizer. The values $T_\perp$ and $T_\parallel$ depend on the sample thickness, on the droplet size and on the matching and mismatching of the refractive indices. Again, rotation of the optical axis of the film between $\psi_1 = \alpha + \theta$ and $\psi_2 = \alpha - \theta$ results in a light modulation ΔI which depends on the tilt angle θ and on the azimuthal orientation α of the sheared PDLC film with respect to the polarizer.

$$\Delta I(\alpha, \theta) = \tfrac{1}{2} I_0 (T_\perp - T_\parallel) \sin 2\alpha \sin 2\theta. \tag{16}$$

Here, optimum contrast for the scattering device is given for $\alpha = \theta = 45^\circ$ (see figure 11 (*f*)), as opposed to $\alpha = \theta = 22{\cdot}5^\circ$ for effects using the liquid crystal as a wave plate (see figure 11 (*e*)). Similarly to the effect of helical unwinding, switching times of about 200 μs and a linear relation between the transmitted intensity and the applied voltage have been reported for the scattering PDFLC display [117].

6. Conclusions

Almost a century after the discovery of mesophases, droplets of liquid crystals dispersed in a polymer film have found recent attraction due to both the possibility of applications and interesting physical questions. The rapid progress in this field opens a lot of questions for basic research and opportunities for further material developments and additional applications.

The competing influences of elastic forces, anchoring strength and external fields cause complicated director patterns characterized by corresponding disclinations. The behaviour of radial and axial nematic droplets in electric fields has been well investigated, but recent studies have been devoted to *twisted radial* and *twisted bipolar* structures [140, 142] which might also need to be considered in order to explain the switching behaviour of nematic PDLC displays. Certainly, the structures of *cholesteric and chiral smectic droplets* under various anchoring conditions have to be explored in more detail. For basic investigations like the determination of the saddle-splay elastic constant K_{24} [18] or the anchoring energy W_0 [19], a *cylindrical geometry* may be most convenient. Thus, liquid crystals have been studied in capillary tubes [179–182], porous membranes [18, 19, 183–184], and closed cylindrical cavities [185, 186]. Recent work on liquid crystals in cylinders has been devoted to biaxiality in nematics [187], to curvature-induced anchoring transitions [188], to the optical determination of K_{33}/K_{11} [189] and to the behaviour of cholesteric liquid crystals [190]. Large cylindrical cavities may also be a suitable model system to explore the basic principles of PDFLC displays in more detail. Recently, finite size effects on the order parameter and the stability of liquid crystals have also been studied in aerogels which exhibit *pores with random size and shape* [191].

With respect to applications, nematic PDLCs are already extensively used, but the investigation of dispersed cholesteric and chiral smectic liquid crystals has just started, and these systems have to be further optimized. With respect to ferroelectric liquid crystals, the goal might be to achieve true long-time bistability for appropriate cell parameters and curing conditions, or to improve the performance of the PDFLC scattering display [117]. Apart from PDFLC-based applications, a new approach which makes use of a large interface/volume ratio is the dispersion of small particles or polymers in a liquid crystal. The *filled nematic phase* [192], which incorporates a dispersion of pyrogenic silica particles in a nematic phase, has been very effectively used to build an optically addressable storage device. *Anisotropic gels* [104–108] and the most recently invented *liquid crystal pastes* [193] contain a large fraction of the

monomer liquid crystal and only a small amount of a mesogenic polymer network which can be formed by *in situ* photopolymerization in a uniformly aligned state. The latter systems are useful for haze-free transmissive displays [104, 105, 108] and bistable reflective colour displays [107]. The synthesis of suitable mesogenic polymer precursors is a challenge for future preparative work. Finally, the addition of a polymer to monomer liquid crystals may also improve the properties of conventional displays, as demonstrated by the *volume-stabilized ferroelectric liquid crystal display* [17].

The author would like to thank P. P. Crooker, G. Heppke, B. Liu, H. Molsen and F. Xu for many hints and for exciting collaborations. Illuminating discussions with J. W. Doane and the liquid crystal group at Kent State University are gratefully acknowledged, as well as the assistance by J. W. Doane, P. S. Drzaic, T. Gunjima, A. M. Lackner, and G. W. Smith who kindly agreed to the reproduction of their figures. Financially, this work was supported by the Deutsche Forschungsgemeinschaft (Sfb 335).

References

[1] Reinitzer, F., 1888, *Mh. Chem.*, **9**, 421.
[2] Lehmann, O., 1908, *Flüssige Kristalle und die Theorien des Lebens* (Verlag Johann Ambrosius Barth, Leipzig).
[3] Friedel, M. G., 1922, *Annls. Phys.*, Série **9**, **18**, 273.
[4] McDonnell, D. G., 1987, *Thermotropic Liquid Crystals* (Critical Reports on Applied Chemistry, Vol. 22), edited by G. W. Gray (John Wiley & Sons), p. 120.
[5] Doane, J. W., Golemme, A., West, J. L., Whitehead, J. B., and Wu, B.-G., 1988, *Molec. Crystals liq. Crystals*, **165**, 511.
[6] Doane, J. W., 1990, *Liquid Crystals—Applications and Uses*, edited by B. Bahadur, Vol. 1 (World Scientific Publishing), p. 361.
[7] Fergason, J. L., 1984, United States Patent No. 4435047.
[8] Doane, J. W., Vaz, N., Wu, B.-G., and Žumer, S., 1986, *Appl. Phys. Lett.*, **48**, 269.
[9] Crooker, P. P., and Yang, D. K., 1990, *Appl. Phys. Lett.*, **57**, 2529.
[10] Kitzerow, H.-S., Molsen, H., and Heppke, G., 1992, *Appl. Phys. Lett.*, **60**, 3093.
[11] Skarp, K., and Handschy, M. A., 1988, *Molec. Crystals liq Crystals*, **165**, 439.
[12] Castellano, J. A., 1988, *Molec. Crystals liq. Crystals*, **165**, 389.
[13] Craighead, H. G., Cheng, J., and Hackwood, S., 1982, *Appl. Phys. Lett.*, **40**, 22.
[14] Schadt, M., 1988, *Molec. Crystals liq. Crystals*, **165**, 405.
[15] Lackner, A. M., Margerum, J. D., Ramos, E., Smith, W. H., and Lim, K. C., 1990, U.S. Patent No. 4944576.
[16] Margerum, J. D., Lackner, A. M., Ramos, E., Lim, K.-C., and Smith, W. H., 1989, *Liq. Crystals*, **5**, 1477.
[17] Pirš, J., Blinc, R., Marin, B., Muševič, I., Pirš, S., Žumer, S., and Doane, J. W., 1992, *14th International Liquid Crystal Conference*, Pisa (Italy), Poster C-P89.
[18] Allender, D. W., Crawford, G. P., and Doane, J. W., 1991, *Phys. Rev. Lett.*, **67**, 1442.
[19] Crawford, G. P., Allender, D. W., Doane, J. W., Vilfan, M., and Vilfan, I., 1991, *Phys. Rev. A*, **44**, 2570.
[20] Žumer, S., and Kralj, S., 1992, *Liq. Crystals*, **12**, 613.
[21] Crawford, G. P., Yang, D. K., Žumer, S., Finotello, D., and Doane, J. W., 1991, *Phys. Rev. Lett.*, **66**, 723.
[22] Crawford, G. P., Stannarius, R., and Doane, J. W., 1991, *Phys. Rev. A*, **44**, 2558.
[23] Poniewierski, A., and Sluckin, T. J., 1987, *Liq. Crystals*, **2**, 281.
[24] Golemme, A., Žumer, S., Allender, D. W., and Doane, J. W., 1988, *Phys. Rev. Lett.*, **61**, 2937.
[25] Kralj, S., Žumer, S., and Allender, D. W., 1991, *Phys. Rev. A*, **43**, 2943.
[26] Gilli, J. M., and Kamayé, M., 1992, *Liq. Crystals*, **12**, 545.
[27] Radian-Guenebaud, M., and Sixou, P., 1992, *Molec. Crystals liq. Crystals*, **220**, 53.
[28] Stein, D. L., Pisarski, R. D., and Anderson, P. W., 1978, *Phys. Rev. Lett.*, **40**, 1269.

[29] MERMIN, N. D., 1979, *Rev. mod. Phys.*, **51**, 591.
[30] VOLOVIK, G. E., 1979, *Sov. Phys. JETP Lett.*, **28**, 59.
[31] DRZAIC, P. S. (Editor), 1991, *Liquid Crystal Devices and Materials* (Proc. SPIE, Vol. 1455).
[32] DRZAIC, P. S., and EFRON, U. (editors), 1992, *Liquid Crystal Materials, Devices, and Applications* (Proc. SPIE, Vol. 1665).
[33] MORREALE, J. (editor), 1992, *SID Dig. Tech. Papers*, Vol. XXIII.
[34] CANDAU, S., LE ROY, P., and DEBEAUVAIS, F., 1973, *Molec. Crystals liq. Crystals*, **23**, 283.
[35] KURIK, M. V., and LAVRENTOVICH, O. D., 1982, *Sov. Phys. JETP Lett.*, **35**, 444.
[36] BOULIGAND, Y., and LIVOLANT, F., 1984, *J. Phys., Paris*, **45**, 1899.
[37] DRZAIC, P. S., 1988, *Molec. Crystals liq. Crystals*, **154**, 289.
[38] KOVAL'CHUK, A. V., KURIK, M. V., LAVRENTOVICH, O. D., and SERGAN, V. V., 1988, *Sov. Phys. JETP*, **67**, 1065.
[39] VOLOVIK, G. E., and LAVRENTOVICH, O. D., 1983, *Sov. Phys. JETP*, **58**, 1159.
[40] PRESS, M. J., and ARROT, A. S., 1974, *Phys. Rev. Lett.*, **33**, 403.
[41] PRESS, M. J., and ARROT, A. S., 1975, *J. Phys., Paris, Coll.*, **36**, C1-177.
[42] BODNAR, V. G., LAVRENTOVICH, O. D., and PERGAMENSHCHIK, V. M., 1992, *Sov. Phys. JETP*, **74**, 60.
[43] FERGASON, J. L., 1986, U.S. Patent 4 616 903.
[44] DRZAIC, P. S., 1986, *J. appl. Phys.*, **60**, 2142.
[45] DRZAIC, P. S., 1988, *Liq. Crystals*, **3**, 1543.
[46] DRZAIC, P. S., 1989, *Proc. SPIE*, **1080**, 11.
[47] DRZAIC, P. S., and MULLER, A., 1989, *Liq. Crystals*, **5**, 1467.
[48] DRZAIC, P. S., WILEY, R., and MCCOY, J., 1989, *Proc. SPIE*, **1080**, 41.
[49] DRZAIC, P. S., 1991, *Molec. Crystals liq. Crystals*, **198**, 61.
[50] MONTGOMERY, G. P., 1989, *Proc. SPIE*, **1080**, 242.
[51] REAMEY, R. H., MONTOYA, W., and WARTENBERG, M., 1991, *Proc. SPIE*, **1455**, 39.
[52] DRZAIC, P. S., and GONZALES, A. M., 1992, *Molec. Crystals liq. Crystals*, **222**, 11.
[53] DRZAIC, P. S., GONZALES, A. M., JONES, P., and MONTOYA, W., 1992, *SID 92 Dig.*, p. 571.
[54] APHONIN, O. A., PANINA, YU. V., PRAVDIN, A. B., and YAKOVLEV, D. A., 1992, *14th International Liquid Crystal Conference*, Pisa (Italy), poster L-P14.
[55] ZAPLO, O., STUMPE, J., SEEBOTH, A., and HERMEL, H., 1992, *Molec. Crystals liq. Crystals*, **213**, 153.
[56] DOANE, J. W., CHIDISHIMO, G., and VAZ, N. A., 1987, U.S. Patent No. 4 688 900.
[57] VAZ, N. A., and MONTGOMERY, G. P., 1987, *J. appl. Phys.*, **62**, 3161.
[58] MONTGOMERY, G. P., and VAZ, N. A., 1987, *Appl. Optics*, **24**, 738.
[59] SIMONI, F., CIPPARONE, G., and UMETON, C., 1990, *Appl. Phys. Lett.*, **57**, 1949.
[60] WU, B.-G., WEST, J. L., and DOANE, J. W., 1987, *J. appl. Phys.*, **62**, 3925.
[61] SEEKOLA, D., and KELLY, J., 1991, *Proc. SPIE*, **1455**, 19.
[62] WEST, J. L., 1988, *Molec. Crystals liq. Crystals*, **157**, 427.
[63] DOANE, J. W., WEST, J. L., PIRŚ, J., ŽUMER, S., and BLINC, R., 1988, *Proc. SPIE*, **958**, 94.
[64] ERDMANN, J., DOANE, J. W., ŽUMER, S., and CHIDICHIMO, G., 1989, *Proc. SPIE*, **1080**, 32.
[65] WEST, J. L., TAMURA-LIS, W., and ONDRIS, R., 1989, *Proc. SPIE*, **1080**, 48.
[66] MONTGOMERY, G. P., WEST, J. L., and TAMURA-LIS, W., 1991, *Proc. SPIE*, **1455**, 45.
[67] CHIDICHIMO, G., ARABIA, G., GOLEMME, A., and DOANE, J. W., 1989, *Liq. Crystals*, **5**, 1443.
[68] DOANE, J. W., WEST, J. L., WHITEHEAD, J. B., and FREDLEY, D. S., 1991, *SID 91 Digest*, 133.
[69] CHIEN, L. C., LIN, C., FREDLEY, D. S., and MCCARGAR, J. W., 1992, *Macromolecules*, **25**, 1.
[70] ALOE, R., CHIDICHIMO, G., and GOLEMME, A., 1991, *Molec. Crystals liq. Crystals*, **203**, 9.
[71] SMITH, G. W., VENTOURIS, G. M., and WEST, J. L., 1992, *Molec. Crystals liq. Crystals*, **213**, 11.
[72] VAZ, N. A., SMITH, G. W., VANSTEENKISTE, T. H., and MONTGOMERY, G. P., 1991, *Proc. SPIE*, **1455**, 110.
[73] ERDMANN, J. H., ŽUMER, S., and DOANE, J. W., 1990, *Phys. Rev. Lett.*, **64**, 1907.
[74] ERDMANN, J. H., ŽUMER, S., WAGNER, B. G., and DOANE, J. W., 1990, *Proc. SPIE*, **1257**, 68.
[75] VAZ, N. A., SMITH, G. W., and MONTGOMERY, G. P., 1987, *Molec. Crystals liq. Crystals*, **146**, 1.
[76] MONTGOMERY, G. P., VAZ, N. A., and SMITH, G. W., 1988, *Proc. SPIE*, **958**, 104.
[77] LACKNER, A. M., MARGERUM, J. D., RAMOS, E., WU, S. T., and LIM, K. C., 1988, *Proc. SPIE*, **958**, 73.

[78] LACKNER, A. M., MARGERUM, J. D., RAMOS, E., and LIM, K. C., 1989, *Proc. SPIE*, **1080**, 53.
[79] LACKNER, A. M., RAMOS, E., and MARGERUM, J. D., 1989, *Proc. SPIE*, **1080**, 267.
[80] GUNJIMA, T., KUMAI, H., TSUCHIYA, S., and MASUDA, K., 1988, European Patent No. 0 272 585.
[81] MUCHA, M., 1991, *Colloid Polym. Sci.*, **269**, 1111.
[82] YAMAGUCHI, R., and SATO, S., 1991, *Jap. J. appl. Phys.*, **30**, L-616.
[83] VAZ, N. A., SMITH, G. W., and MONTGOMERY, G. P., 1990, *Proc. SPIE*, **1257**, 9.
[84] NOLAN, P., and COATES, D., 1991, *Molec. Crystals liq. Crystals Lett.*, **8**, 75.
[85] SMITH, G. W., 1991, *Molec. Crystals liq. Crystals*, **196**, 89.
[86] MARGERUM, J. D., LACKNER, A. M., ERDMANN, J. H., and SHERMAN, E., 1991, *Proc. SPIE*, **1455**, 27.
[87] LIN, Z., SLUSS, J. J., BATCHMAN, T. E., HEAVIN, S. D., and FUNG, B. M., 1992, *Molec. Crystals liq. Crystals*, **220**, 29.
[88] NOLAN, P., TILLIN, M., and COATES, D., 1992, *Molec. Crystals liq. Crystals Lett.*, **8**, 129.
[89] NOLAN, P., TILLIN, M., and COATES, D., 1993, *Liq. Crystals*, **14**, 339.
[90] TILLIN, M., COATES, D., and NOLAN, P., 1992, Poster presented at the *14th International Liquid Crystal Conference*, Pisa (to be published).
[91] KELLY, J. R., and WU, W., 1993, *Liq. Crystals*, **14**, 1683.
[92] ZANOTTI, A., and GRULER, H., 1992 (private communication).
[93] MONTGOMERY, G. P., VAZ, N. A., and SMITH, G. W., 1993, *Molec. Crystals liq. Crystals*, **225**, 131.
[94] JAIN, S. C., and THAKUR, R. S., 1992, *Appl. Phys. Lett.*, **61**, 1641.
[95] ONDRIS-CRAWFORD, R., BOYKO, E. P., WAGNER, B. G., ERDMANN, J. H., ŽUMER, S., and DOANE, J. W., 1991, *J. appl. Phys.*, **69**, 6380.
[96] WU, B.-G., ERDMANN, J. H., and DOANE, J. W., 1989, *Liq. Crystals*, **5**, 1453.
[97] JAIN, S. C., ROUT, D. K., and CHANDRA, S., 1990, *Molec. Crystals liq. Crystals*, **188**, 251.
[98] ROUT, D. K., and JAIN, S. C., 1991, *Jap. J. appl. Phys.*, **30**, L-1412.
[99] HEAVIN, S. D., FUNG, B. M., MEARS, R. B., SLUSS, J. J., and BATCHMAN, Th. E., 1991, *Proc. SPIE*, **1455**, 12.
[100] JAIN, S. C., and ROUT, D. K., 1991, *J. appl. Phys.*, **70**, 6988.
[101] MCCARGAR, J. W., DOANE, J. W., WEST, J. L., and ANDERSON, Th. W., 1991, *Proc. SPIE*, **1455**, 54.
[102] WEST, J. L., KELLY, J. R., JEWELL, K., and JI, Y., 1992, *Appl. Phys. Lett.*, **60**, 3238.
[103] PARMAR, D. S., and SINGH, J. J., 1993, *Molec. Crystals liq. Crystals*, **225**, 183.
[104] HIKMET, R. A. M., 1990, *J. appl. Phys.*, **68**, 4406.
[105] HIKMET, R. A. M., 1992, *Molec. Crystals liq. Crystals*, **213**, 117.
[106] HIKMET, R. A. M., and ZWERVER, B. H., 1991, *Molec. Crystals liq. Crystals*, **200**, 197.
[107] YANG, D. K., and DOANE, J. W., 1992, *SID 92 Dig.*, p. 759.
[108] YANG, D. K., CHIEN, L.-C., and DOANE, J. W., 1992, *Appl. Phys. Lett.*, **60**, 3102.
[109] STANNARIUS, R., CRAWFORD, G. P., CHIEN, L. C., and DOANE, J. W., 1991, *J. appl. Phys.*, **70**, 135.
[110] OTÓN, J. M., SERRANO, A., SERNA, C. J., and LEVY, D., 1991, *Liq. Crystals*, **10**, 733.
[111] LEVY, D., PENA, J. M. S., SERNA, C. J., and OTÓN, J. M., 1992, *J. non-crystalline Solids*, **147 & 148**, 646.
[112] Licrilite$^{(R)}$ liquid crystal mixtures, Merck Ltd., Poole, England.
[113] MA, Y.-D., WU, B.-G., and XU, G., 1990, *Proc. SPIE*, **1257**, 46.
[114] KITZEROW, H.-S., XU, F., and CROOKER, P. P., 1992, *Liq. Crystals*, **12**, 1019.
[115] HEPPKE, G., KITZEROW, H.-S., and MOLSEN, H., 1993, *Mol. Crystals liq. Crystals Lett.* (in the press).
[116] KITZEROW, H.-S., MOLSEN, H., and HEPPKE, G., 1992, *Polym. Adv. Tech.*, **3**, 231.
[117] ZYRYANOV, V. YA., SMORGON, S. L., and SHABANOV, V. F., 1992, *SID 92 Dig.*, p. 776.
[118] WILLIAMS, P. A., CLARK, N. A., ROS, M. B., WALBA, D. M., and WAND, M. D., 1991, *Ferroelectrics*, **121**, 143.
[119] KOMITOV, L., LAGERWALL, S. T., STEBLER, B., ALOE, R., CHIDICHIMO, G., CLARK, N. A., and WALBA, D., 1992, *14th International Liquid Crystal Conference*, Pisa (Italy), lecture J-SC7.
[120] MOLSEN, H., KITZEROW, H.-S., and HEPPKE, G., 1992, *Jap. J. appl. Phys.*, **31**, L-1083.
[121] DRZAIC, P. S., 1991, *Proc. SPIE*, **1455**, 255.

[122] Smith, G. W., and Vaz, N. A., 1988, *Liq. Crystals*, **3**, 543.
[123] Smith, G. W., 1990, *Molec. Crystals liq. Crystals*, **180B**, 201.
[124] Kim, J. Y., Cho, C. H., Palffy-Muhoray, P., Mustafa, M., and Kyu, T., 1991, *Technical Reports of the ALCOM Symposium*, Cuyahega Falls, Ohio (USA).
[125] Kim, J. Y., and Palffy-Muhoray, P., 1991, *Molec. Crystals liq. Crystals*, **203**, 93.
[126] Konynenburg, P. van, Wipfler, R., and Smith, J. L., 1989, *Proc. SPIE*, **1080**, 62.
[127] Fergason, J. L., 1987, U.S. Patent No. 4 693 557.
[128] Takizawa, K., Kikuchi, H., and Fujikake, 1991, *SID 91 Dig.*, 250.
[129] Przyrembel, G., and Yilmaz, S., *3rd International Conference on Electrical, Optical and Acoustic Properties of Polymers (EOA III)*, London, England.
[130] Simoni, F., Bloisi, F., Duca, D., and Vicari, L., 1992, *Molec. Crystals liq. Crystals*, **212**, 279.
[131] Li, L., Yuan, H. J., and Palffy-Muhoray, P., 1991, *Molec. Crystals liq. Crystals*, **198**, 239.
[132] Hirai, Y., Niiyama, S., Kumai, H., and Gunjima, T., 1990, *Rep. Res. Lab. Asahi Glass Co.*, **40**, 285.
[133] Doane, J. W., 1991, *Mater. Res. Soc. Bull.*, **XVI (1)**, 22.
[134] Žumer, S., and Doane, J. W., 1986, *Phys. Rev.* A, **34**, 3373.
[135] Žumer, S., 1988, *Phys. Rev.* A, **37**, 4006.
[136] Heilmeier, G. H., Castellano, J. A., and Zanoni, L. A., 1969, *Molec. Crystals liq. Crystals*, **8**, 293.
[137] Dubois-Violette, E., and Parodi, O., 1969, *J. Phys., Paris, Coll.*, **30**, C4–57.
[138] Williams, R. D., 1986, *J. Phys.* A, **19**, 3211.
[139] Lavrentovich, O. D., and Sergan, V. V., 1990, *Nuovo Cim.*, **12**, 1219.
[140] Xu, F., Kitzerow, H.-S., and Crooker, P. P., 1994, *Phys. Rev.* E (in the press).
[141] Le Roy, P., Debeauvais, F., Candau, S., and Guinier, M. A., 1972, *C. r. hebd Séanc. Acad. Sci. Paris*, B, **274**, 419.
[142] Xu, F., Kitzerow, H.-S., and Crooker, P. P., 1993, *Phys. Rev.* A, **46**, 6535.
[143] Mermin, N. D., 1977, *Quantum Fluids and Solids*, edited by S. B. Trickey, E. Adams and J. Duffy (Plenum).
[144] Lavrentovich, O. D., and Terent'ev, E. M., 1986, *Sov. Phys. JETP*, **64**, 1237.
[145] Kralj, S., and Žumer, S., 1992, *Phys. Rev.* A, **45**, 2461.
[146] Žumer, S., Kralj, S., and Bezić, J., 1992, *Molec. Crystals liq. Crystals*, **212**, 163.
[147] Lavrentovich, O. D., Marusiy, T., Resnikov, Yu., and Sergan, V., 1990, *Molec. Crystals liq. Crystals*, **192**, 75.
[148] Chiccoli, C., Pasini, P., Semeria, F., and Zannoni, C., 1992, *Molec. Crystals liq. Crystals*, **212**, 197.
[149] Kilian, A., 1993, *Liq. Crystals*, **14**, 1189.
[150] Kilian, A., and Hess, S., 1989, *Z. Naturf.* (*a*), **44**, 693.
[151] Golemme, A., Žumer, S., Doane, J. W., and Neubert, M. E., 1988, *Phys. Rev.* A, **37**, 559.
[152] Kralj, S., Vilfan, M., and Žumer, S., 1989, *Liq. Crystals*, **5**, 1489.
[153] Shurcliff, W. A., 1962, *Polarized Light* (Harvard University Press).
[154] Kitzerow, H.-S., and Crooker, P. P., 1991, *Ferroelectrics*, **122**, 183.
[155] Kitzerow, H.-S., Crooker, P. P., and Heppke, G., 1992, *Liq. Crystals*, **12**, 49.
[156] Kitzerow, H.-S., and Crooker, P. P., 1993, *J. Phys. II, France*, **3**, 719.
[157] Kitzerow, H.-S., Rand, J., and Crooker, P. P., 1992, *J. Phys. II, Paris*, **2**, 227.
[158] Seuron, P., and Solladie, G., 1979, *Molec. Crystals liq. Crystals*, **56**, 1.
[159] Robinson, C., 1956, *Trans. Faraday Soc.*, **52**, 571.
[160] Robinson, C., Ward, J. C., and Beever, R. B., 1958, *Discuss. Faraday Soc.*, **25**, 29.
[161] Robinson, C., 1966, *Molec. Crystals liq. Crystals*, **2**, 71.
[162] Bezić, J., and Žumer, S., 1992, *Liq. Crystals*, **11**, 593.
[163] Patel, D. L., and DuPré, D. B., 1980, *J. polym. Sci.*, **18**, 1599.
[164] Kitzerow, H.-S., and Crooker, P. P., 1993, *Liq. Crystals*, **13**, 31.
[165] de Gennes, P. G., 1968, *Solid St. Commun.*, **6**, 163.
[166] Yang, D. K., and Crooker, P. P., 1991, *Liq. Crystals*, **9**, 245.
[167] Kitzerow, H.-S., and Crooker, P. P., 1992, *Liq. Crystals*, **11**, 561.
[168] Quigley, J. R., and Benton, W., 1977, *Molec. Crystals liq. Crystals*, **42**, 43.
[169] Bezić, J., Žumer, S., and Bajc, J., 1993, Poster presented at the *European Conference on Liquid Crystals*, Flims (to be published).

[170] CLARK, N. A., and LAGERWALL, S. T., 1980, *Appl. Phys. Lett.*, **36,** 899.
[171] GRAY, G. W., and GOODBY, J. W., 1984, *Smectic Liquid Crystals—Textures and Structures* (Leonard Hill).
[172] MEYER, R. B., LIÉBERT, L., STRZELECKI, L., and KELLER, P., 1975, *J. Phys., Paris*, **36,** L-69.
[173] MEYER, R. B., 1977, *Molec. Crystals liq. Crystals*, **40,** 33.
[174] GAROFF, S., and MEYER, R. B., 1977, *Phys. Rev. Lett.*, **36,** 848.
[175] TAKEZOE, H., LEE, J., CHANDANI, A. D. L., GORECKA, E., OUCHI, Y., and FUKUDA, A., 1991, *Ferroelectrics*, **114,** [187]/675.
[176] MARTINOT-LAGARDE, Ph., 1976, *J. Phys. Paris*, **37,** C3-129.
[177] MIYATSO, K., ABE, S., TAKEZOE, H., FUKUDA, A., and KUZE, E., 1983, *Jap. J. appl. Phys.*, **22,** L-661.
[178] MOLSEN, H., and KITZEROW, H.-S., 1994, *J. appl. Phys.* (scheduled for the January issue).
[179] WILLIAMS, C. E., PIERANSKI, P., and CLADIS, P. E., 1972, *Phys. Rev. Lett.*, **29,** 90.
[180] WILLIAMS, C. E., CLADIS, P. E., and KLÉMAN, M., 1973, *Molec. Crystals liq. Crystals*, **21,** 355.
[181] CLADIS, P. E., WHITE, A. E., and BRINKMAN, W. F., 1979, *J. Phys., Paris*, **40,** 325.
[182] VILFAN, I., VILFAN, M., and ŽUMER, S., 1991, *Phys. Rev.* A, **43,** 6875.
[183] KUZMA, M., and LABES, M. M., 1983, *Molec. Crystals liq. Crystals*, **100,** 103.
[184] CRAWFORD, G. P., STEELE, L. M., ONDRIS-CRAWFORD, R., IANNACCHIONE, G. S., YEAGER, C. J., DOANE, J. W., and FINOTELLO, D., 1992, *J. chem. Phys.*, **96,** 7788.
[185] LIANG, B.-J., and CHEN, S.-H., 1991, *Jap. J. appl. Phys.* B, **30,** L-1955.
[186] LIANG, B.-J., and CHEN, S.-H., 1992, *J. appl. Phys.*, **71,** 2189.
[187] LIU, J., and SAUPE, A., 1993, *Proceedings of the V International Meeting on Optics of Liquid Crystals*, Lake Balaton (to be published).
[188] ONDRIS-CRAWFORD, R. J., CRAWFORD, G. P., ŽUMER, S., and DOANE, J. W., 1993, *Phys. Rev. Lett.*, **70,** 194.
[189] CRAWFORD, G. P., MICHELTREE, J. A., BOYKO, E. P., FRITZ, W., ŽUMER, S., and DOANE, J. W., 1992, *Appl. Phys. Lett.*, **60,** 3226.
[190] LIU, B., XU, F., KITZEROW, H.-S., and CROOKER, P. P., 1994 (to be published).
[191] BELLINI, T., CLARK, N. A., MUZNY, C. D., WU, L., GARLAND, C. W., SCHAEFER, D. W., and OLIVER, B. J., 1992, *Phys. Rev. Lett.*, **69,** 788.
[192] KREUZER, M., TSCHUDI, TH., and EIDENSCHINK, R., 1992, *Molec. Crystals liq. Crystals*, **223,** 219.
[193] JÁKLI, A., KIM, D. R., CHIEN, L. C., and SAUPE, A., 1992, *J. appl. Phys.*, **72,** 3161.